We did not detect the association of Mal with PI(3)K-p85 in unstimulated neutrophils from healthy controls; however, we did observe this association in Btk-deficient neutrophils before stimulation with PMA (Fig. 6d). Moreover, confocal fluorescence microscopy showed targeting of the PI(3)K-p85–Mal complex to the membrane in the absence of Btk, whereas we observed the complex at the membrane after stimulation with PMA in the presence of Btk (Fig. 6e). In addition, most of the PI(3)K-p85 and Mal was present in the membrane fraction in neutrophils from patients with XLA (Fig. 6f). These data suggested that Btk in resting neutrophils was involved in confining Mal to the cytoplasm.

The mode of the Btk-Mal association

Btk phosphorylates Mal at Tyr86, Tyr106 and Tyr187, and the Btk-Mal interaction requires Pro125, Tyr86, Tyr106 and Tyr159 in Mal, whereas the critical site in Btk for this association remains unknown[21,22]. To clarify the region of Btk required for the cytoplasmic Btk-Mal association, we generated various Btk deletion mutants fused to histidine-tagged Hph-1 (Fig. 7a) and assessed their binding to Mal (Fig. 7).

We incubated nickel bead–bound recombinant proteins with the cytoplasmic fraction of control neutrophils and evaluated the associations by immunoblot analysis with anti-Mal. Full-length Btk effectively bound to cytoplasmic Mal prepared from control neutrophils, but a control fusion of histidine-tagged Hph-1 and enhanced green fluorescent protein (eGFP) did not. Btk with deletion of the kinase domain almost completely lost the ability to interact with Mal, and Btk with deletion of the PH domain showed less binding to Mal. In contrast, recombinant proteins lacking the Tec homology domain, the Src homology 3 domain or the Src homology 2 domain had slightly greater capacity to associate with Mal (Fig. 7b,d). Other truncated Btk recombinant proteins without either the PH domain or kinase domain failed to bind to Mal (Fig. 7c,d), which suggested that both the PH domain and kinase domain are critical for the Btk-Mal interaction.

PTKs associate with Mal and regulate PI(3)K activation

The precise mechanism of PI(3)K activation triggered by membrane-associated Mal is largely unknown. As several PTKs were phosphorylated
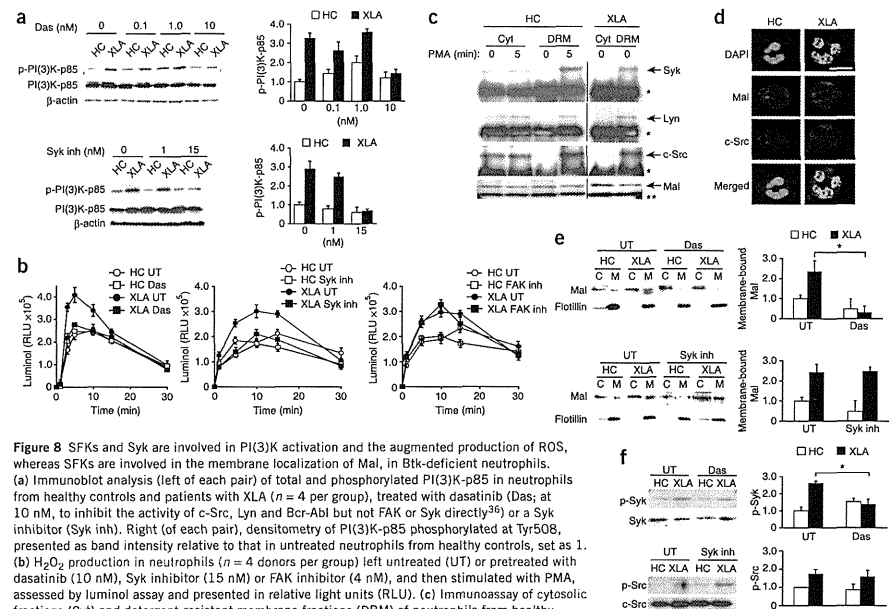

Figure 8 SFKs and Syk are involved in PI(3)K activation and the augmented production of ROS, whereas SFKs are involved in the membrane localization of Mal, in Btk-deficient neutrophils. (a) Immunoblot analysis (left of each pair) of total and phosphorylated PI(3)K-p85 in neutrophils from healthy controls and patients with XLA (n = 4 per group), treated with dasatinib (Das; at 10 nM, to inhibit the activity of c-Src, Lyn and Bcr-Abl but not FAK or Syk directly[36]) or a Syk inhibitor (Syk inh). Right (of each pair), densitometry of PI(3)K-p85 phosphorylated at Tyr508, presented as band intensity relative to that in untreated neutrophils from healthy controls, set as 1. (b) H_2O_2 production in neutrophils (n = 4 donors per group) left untreated (UT) or pretreated with dasatinib (10 nM), Syk inhibitor (15 nM) or FAK inhibitor (4 nM), and then stimulated with PMA, assessed by luminol assay and presented in relative light units (RLU). (c) Immunoassay of cytosolic fractions (Cyt) and detergent-resistant membrane fractions (DRM) of neutrophils from healthy controls and patients with XLA, left untreated (0) or treated for 5 min with PMA (5), followed by immunoprecipitation with anti-Mal and immunoblot analysis with anti-Syk, anti-Lyn, anti-c-Src or anti-Mal. *, immunoglobulin heavy chain; **, immunoglobulin light chain. (d) Confocal microscopy of neutrophils from healthy controls and patients with XLA (n = 3 per group), stained with anti-Mal (red) and anti-c-Src (blue) and counterstained with DAPI. Original magnification, ×600; scale bar, 10 μm. (e) Immunoblot analysis (left) of Mal in the cytoplasm (C) and membrane (M) of neutrophils from healthy controls and patients with XLA (n = 5 per group), left untreated or treated as in a. Right, quantification of results for Mal (left), presented relative to that of flotillin in the membrane fraction of neutrophils from healthy controls, set as 1. *P = 0.0024 (Student's t-test). (f) Immunoblot analysis of total Syk and Syk phosphorylated at Tyr524 and Tyr525 (top left) and of total c-Src and c-Src phosphorylated at Tyr416 (bottom left) in neutrophils from healthy controls and patients with XLA, left untreated or treated with dasatinib (top left) or Syk inhibitor (bottom left). Right, quantification of band intensity relative to that of β-actin in untreated neutrophils from healthy controls, set as 1. *P = 0.013 (Student's t-test). Data are from four (a) or five (f) independent experiments, are from one representative of four independent experiments (c) or are representative of four experiments (b,e) or three experiments (c; mean and s.d. in a,b,e,f).

---

in resting neutrophils from patients with XLA, we first used PTK inhibitors to investigate whether PTKs were involved in the PI(3)K activation. Inhibition of the activity of Src-family kinases (SFKs) by dasatinib (at a concentration of 10 nM)[36] led to normalized phosphorylation of PI(3)K-p85 in neutrophils derived from patients with XLA. Similarly, a Syk inhibitor (at a concentration of 15 nM)[37] but not a FAK inhibitor (at a concentration of 10 nM)[38] abrogated the hyperphosphorylation of PI(3)K (Fig. 8a and data not shown). The lower PI(3)K phosphorylation produced by dasatinib or the Syk inhibitor was accompanied by normalized production of ROS (Fig. 8b), which indicated that SFKs and Syk were involved in the augmented production of ROS in neutrophils from patients with XLA.

The findings noted above prompted us to determine whether the activated PTKs associated with Mal. SFKs are recruited to lipid rafts when activated for the assembly of signal components[39,40]. Coprecipitation assays showed that Lyn, c-Src and Syk interacted with Mal at the rafts of Btk-deficient neutrophils before stimulation (Fig. 8c). We also observed the colocalization of Mal and c-Src at the membrane by confocal fluorescence microscopy (Fig. 8d). We observed the interaction at the rafts of control neutrophils only after stimulation with PMA (Fig. 8c and Supplementary Fig. 6).

SFKs are cytoplasmic kinases and are anchored to the plasma membrane through myristoylation and palmitoylation[39,40]. Coprecipitation assays showed that Lyn, c-Src and Syk were associated with Mal in the cytosol of neutrophils from healthy controls but not in Btk-deficient neutrophils (Fig. 8c). We also confirmed by immunofluorescence staining the presence of c-Src associated with Mal in the cytoplasm but not in the membrane of normal resting neutrophils (Fig. 8d).

We next studied whether the membrane localization of Mal was regulated by SFKs or by Syk. The localization of Mal to the membrane in Btk-deficient neutrophils was diminished to normal amounts in cells treated with dasatinib but not those treated with the Syk inhibitor (Fig. 8e), which suggested that kinase activity of SFKs was required for membrane recruitment or maintenance of membrane-anchoring of Mal. Treatment of neutrophils from patients with XLA with dasatinib resulted in less baseline Syk phosphorylation, whereas incubation with the Syk inhibitor did not abrogate the hyperphosphorylation of c-Src (Fig. 8f), which indicated that Syk was downstream of SFKs in the steady-state signaling cascade of Btk-deficient neutrophils.

Collectively, the data reported above indicated that at least some PTKs associated with Mal together with Btk in the cytoplasm; in the absence of Btk, SFKs and Mal translocated to the membrane. The membrane-recruited PTKs formed a complex with and phosphorylated PI(3)K-p85 (Supplementary Fig. 7). It is still unclear which neutrophil SFK contributes to PI(3)K activation. Our findings may indicate that c-Src (or other SFKs) but not Lyn is (are) directly involved in the PI(3)K activation in Btk-deficient neutrophils; however, the possibility of an indirect contribution of Lyn to the phosphorylation of PI(3)K-p85 cannot be excluded solely by the inhibitor assay.

DISCUSSION

So far, most data have posited Btk as an essential molecule in innate immune responses[12–15,23,25]. Here we have shown that Btk is a negative regulator of signal transduction that leads to activation of NADPH oxidase and a molecule that prevents excessive neutrophil responses. Neutropenia in patients with XLA is usually induced by infection and is observed less often after immunoglobulin supplementation. This phenomenon can most probably be explained by ROS-mediated apoptosis of neutrophils triggered by the engagement of innate receptors and not by abnormal myeloid differentiation.

Our study suggested that Btk serves as a cytosolic component that interacts with Mal to prevent its translocation to the membrane and its interactions with PI(3)K until the appropriate stimulation is received. Both the PH and kinase domains of Btk were necessary for association with cytoplasmic Mal and were important for proper and coordinated initiation of the TLR and TNF receptor responses in human neutrophils. A similar mode of interaction has been demonstrated for the association of Btk with the cell-surface death receptor Fas (CD95) in B cells. Btk associates with Fas via its PH and kinase domains and prevents the interaction of Fas with the Fas-associated death domain and thus serves as a negative regulator of the Fas death-inducing signaling complex[41]. Notably, Btk serves as a negative regulator of apoptosis in both signaling systems.

SFKs were also involved in the baseline activation of PI(3)K in Btk-deficient neutrophils. We detected the association of c-Src, Lyn and Syk with Mal in the membrane raft in the absence of Btk. In addition, localization of Mal to the membrane in Btk-defective neutrophils was dependent on SFKs. These findings may indicate that SFKs serve as a substitute for the function of Btk in guiding the localization of Mal, albeit in an unregulated way. In neutrophils from control subjects, SFKs and Mal were associated in the cytoplasm and localized to the raft after stimulation. The mode of the SFK-Mal interaction remains unclear; however, we speculate that the kinase domain is involved, as SFKs lack a PH domain and the kinase domains of SFKs and Btk share 40–45% homology. Precise mapping of the Mal-binding site in the Btk kinase domain would help to clarify the SFK-Mal association site. Notably, neutrophils had more abundant expression of Mal than did monocytes (data not shown). Our data suggest that Mal is a critical coordinator of the priming signal and that its localization is tightly controlled by Btk.

Limited data indicate a role for PTKs in the production of ROS in neutrophils, particularly in humans. Lyn is reported to be a signaling component of the immunoglobulin receptors FcγRI and FcγRII or the receptor for the hematopoietic cytokine G-CSF, as well as an activator of PI(3)K[30,42], but is also noted for its ability to negatively regulate myeloid-cell signaling through phosphorylation of inhibitory receptors and recruitment of phosphatases[29]. Lyn-deficient neutrophils produce less ROS than Lyn-sufficient neutrophils do after stimulation with G-CSF[30] but show an enhanced respiratory burst after integrin-mediated signaling[29,31]. ROS responses triggered by Aspergillus species are totally dependent on Syk in mouse neutrophils[43]. The phosphorylation at different regulatory sites in Lyn versus c-Src in Btk-deficient neutrophils is notable. However, overall, PTKs in unstimulated neutrophils from patients with XLA seem to function as positive signal regulators. These data, along with our observations, suggest a potential contribution of SFKs and Syk to the early phase of NADPH oxidase activation in human neutrophils.

Activation of TFKs occurs downstream of SFKs in signaling pathways[40]. However, in neutrophils, Btk regulates baseline SFK activation. There are several possible mechanisms to explain how defective Btk is connected to SFK activation. We first speculated that Btk controls SFKs through the activation of negative SFK regulators. We investigated the Src kinase Csk and its regulatory molecule Cbp[44], but found no difference in the expression, localization or phosphorylation of Csk or Cbp (data not shown). As a second possible mechanism, SFKs but not TFKs may have been activated to compensate for Btk function in neutrophils. It is noteworthy that Btk regulates $PtdIns(4,5)P_2$ synthesis, acting as a shuttle to bring type I phosphatidylinositol-4-phosphate 5-kinases to the plasma membrane in B cells[45]. Although the role of Btk in $PtdIns(4,5)P_2$ production in human neutrophils has not been addressed, the generation of $PtdIns(4,5)P_2$ is a critical

step in the activation of NADPH oxidase. SFKs may have directly or indirectly served as a substitute for the function of Btk in neutrophils from patients with XLA. Finally, the cytoplasmic association of SFKs with Mal but without Btk may have resulted in SFK activation and Lyn inhibition. The phosphorylation of SFKs and subsequent modification of Mal by SFKs may have led to the translocation of Mal in the absence of Btk.

Neutrophils from patients with XLA show excessive production of ROS, but neutrophils from mice with X-linked immunodeficiency show poor ROS induction[15]. One possibility that could explain this discrepancy is the difference between mice and humans in the involvement of Btk in the NADPH oxidase pathway. Another possibility is the difference in the contributions of various members of the PI(3)K family to neutrophil activation. The primed production of ROS requires sequential activation of PI(3)Kγ and PI(3)Kδ in humans, whereas the production of ROS is largely dependent on PI(3)Kγ alone in mice[46]. A third possibility is differences in the methods of neutrophil collection from mice and in our study. Neutrophils collected from the peritoneum after treatment with thioglycolate broth may have been stimulated by that treatment[15]. The production of ROS was not augmented or compromised in neutrophils from patients with XLA in one study[26]. That may also have resulted from a relatively harsh isolation technique of hypotonic shock or from non–endotoxin-free conditions (for example, lipopolysaccharide in FBS) at any point of the experiment.

In this study, we have reported that Btk serves as a critical gatekeeper of neutrophil response. Our study suggests that the regulation of neutrophil activation and apoptosis in various human diseases could be achieved by manipulation of Btk. Future studies should explore the role of Btk in controlling the production of ROS and apoptosis of basophils, mast cells and eosinophils. Finally, ROS-mediated induction of apoptosis after suboptimal or optimal stimuli may be worth investigating in immature and precursor cells of the immune reponse to determine the role of Btk in their survival, proliferation and differentiation.

METHODS
Methods and any associated references are available in the online version of the paper at http://www.nature.com/natureimmunology/.

Note: Supplementary information is available on the Nature Immunology website.

1. Flannagan, R.S., Cosio, G. & Grinstein, S. Antimicrobial mechanisms of phagocytes and bacterial evasion strategies. *Nat. Rev. Microbiol.* 7, 355–366 (2009).
2. Nauseef, W.M. How human neutrophils kill and degrade microbes: an integrated view. *Immunol. Rev.* 219, 88–102 (2007).
3. Lambeth, J.D. NOX enzymes and the biology of reactive oxygen. *Nat. Rev. Immunol.* 4, 181–189 (2004).
4. Babior, B.M. NADPH oxidase. *Curr. Opin. Immunol.* 16, 42–47 (2004).
5. Sumimoto, H. Structure, regulation and evolution of Nox-family NADPH oxidases that produce reactive oxygen species. *FEBS J.* 275, 3249–3277 (2008).
6. Fang, F.C. Antimicrobial reactive oxygen and nitrogen species: concepts and controversies. *Nat. Rev. Microbiol.* 2, 820–832 (2004).
7. Singh, A., Zarember, K.A., Kuhns, D.B. & Gallin, J.I. Impaired priming and activation of the neutrophil NADPH oxidase in patients with IRAK4 or NEMO deficiency. *J. Immunol.* 182, 6410–6417 (2009).
8. Woollard, K.J. & Geissmann, F. Monocytes in atherosclerosis: subsets and functions. *Nat. Rev. Cardiol.* 7, 77–86 (2009).
9. Finkel, T. Radical medicine: treating ageing to cure disease. *Nat. Rev. Mol. Cell Biol.* 6, 971–976 (2005).
10. Conley, M.E. *et al.* Genetic analysis of patients with defects in early B-cell development. *Immunol. Rev.* 203, 216–234 (2005).
11. Winkelstein, J.A. *et al.* X-linked agammaglobulinemia: report on a United States registry of 201 patients. *Medicine (Baltimore)* 85, 193–202 (2006).
12. Mohamed, A.J. *et al.* Bruton's tyrosine kinase (Btk): function, regulation, and transformation with special emphasis on the PH domain. *Immunol. Rev.* 228, 58–73 (2009).
13. Gray, P. *et al.* MyD88 adapter-like (Mal) is phosphorylated by Bruton's tyrosine kinase during TLR2 and TLR4 signal transduction. *J. Biol. Chem.* 281, 10489–10495 (2006).
14. Doyle, S.L., Jefferies, C.A., Feighery, C. & O'Neill, L.A. Signaling by Toll-like receptors 8 and 9 requires Bruton's tyrosine kinase. *J. Biol. Chem.* 282, 36953–36960 (2007).
15. Mangla, A. *et al.* Pleiotropic consequences of Bruton tyrosine kinase deficiency in myeloid lineages lead to poor inflammatory responses. *Blood* 104, 1191–1197 (2004).
16. Fiedler, K. *et al.* Neutrophil development and function critically depend on Bruton tyrosine kinase in a mouse model of X-linked agammaglobulinemia. *Blood* 117, 1329–1339 (2011).
17. Conley, M.E. *et al.* Primary B cell immunodeficiencies: comparisons and contrasts. *Annu. Rev. Immunol.* 27, 199–227 (2009).
18. Kerner, J.D. *et al.* Impaired expansion of mouse B cell progenitors lacking Btk. *Immunity* 3, 301–312 (1995).
19. Khan, W.N. *et al.* Defective B cell development and function in Btk-deficient mice. *Immunity* 3, 283–299 (1995).
20. O'Neill, L.A.J. & Bowie, A.G. The family of five: TIR-domain-containing adaptors in Toll-like receptor signalling. *Nat. Rev. Immunol.* 7, 353–364 (2007).
21. Piao, W. *et al.* Tyrosine phosphorylation of MyD88 adapter-like (Mal) is critical for signal transduction and blocked in endotoxin tolerance. *J. Biol. Chem.* 283, 3109–3119 (2008).
22. Jenkins, K.A. & Mansell, A. TIR-containing adaptors in Toll-like receptor signalling. *Cytokine* 49, 237–244 (2010).
23. Taneichi, H. *et al.* Toll-like receptor signaling is impaired in dendritic cells from patients with X-linked agammaglobulinemia. *Clin. Immunol.* 126, 148–154 (2008).
24. Pérez de Diego, R. *et al.* Bruton's tyrosine kinase is not essential for LPS-induced activation of human monocytes. *J. Allergy Clin. Immunol.* 117, 1462–1469 (2006).
25. Horwood, N.J. *et al.* Bruton's tyrosine kinase is required for TLR2 and TLR4-induced TNF, but not IL-6, production. *J. Immunol.* 176, 3635–3641 (2006).
26. Marron, T.U., Rohr, K., Martinez-Gallo, M., Yu, J. & Cunningham-Rundles, C. TLR signaling and effector functions are intact in XLA neutrophils. *Clin. Immunol.* 137, 74–80 (2010).
27. Honda, F. *et al.* Transducible form of p47phox and p67phox compensate for defective NADPH oxidase activity in neutrophils of patients with chronic granulomatous disease. *Biochem. Biophys. Res. Commun.* 417, 162–168 (2012).
28. Dang, P.M. *et al.* A specific p47phox -serine phosphorylated by convergent MAPKs mediates neutrophil NADPH oxidase priming at inflammatory sites. *J. Clin. Invest.* 116, 2033–2043 (2006).
29. Scapini, P., Pereira, S., Zhang, H. & Lowell, C.A. Multiple roles of Lyn kinase in myeloid cell signaling and function. *Immunol. Rev.* 228, 23–40 (2009).
30. Zhu, Q.S. *et al.* G-CSF induced reactive oxygen species involves Lyn-PI3-kinase-Akt and contributes to myeloid cell growth. *Blood* 107, 1847–1856 (2006).
31. Pereira, S. & Lowell, C. The Lyn tyrosine kinase negatively regulates neutrophil integrin signaling. *J. Immunol.* 171, 1319–1327 (2003).
32. Vlahos, C.J., Matter, W.F., Hui, K.Y. & Brown, R.F. A specific inhibitor of phosphatidylinositol 3-kinase, 2-(4-morpholinyl)-8-phenyl-4H-1-benzopyran-4-one (LY294002). *J. Biol. Chem.* 269, 5241–5248 (1994).
33. Sadhu, C., Masinovsky, B., Dick, K., Sowell, C.G. & Staunton, D.E. Essential role of phosphoinositide 3-kinase δ in neutrophil directional movement. *J. Immunol.* 170, 2647–2654 (2003).
34. Morris, A.C. *et al.* C5a-mediated neutrophil dysfunction is RhoA-dependent and predicts infection in critically ill patients. *Blood* 117, 5178–5188 (2011).
35. Santos-Sierra, S. *et al.* Mal connects TLR2 to PI3Kinase activation and phagocyte polarization. *EMBO J.* 28, 2018–2027 (2009).
36. Nam, S. *et al.* Action of the Src family kinase inhibitor, dasatinib (BMS-354825), on human prostate cancer cells. *Cancer Res.* 65, 9185–9189 (2005).
37. Lai, J.Y. *et al.* Potent small molecule inhibitors of spleen tyrosine kinase (Syk). *Bioorg. Med. Chem. Lett.* 13, 3111–3114 (2003).
38. Slack-Davis, J.K. *et al.* Cellular characterization of a novel focal adhesion kinase inhibitor. *J. Biol. Chem.* 282, 14845–14852 (2007).
39. Korade-Mirnics, Z. & Corey, S.J. Src kinase-mediated signaling in leukocytes. *J. Leukoc. Biol.* 68, 603–613 (2000).
40. Bradshaw, J.M. The Src, Syk, and Tec family kinases: distinct types of molecular switches. *Cell. Signal.* 22, 1175–1184 (2010).
41. Vassilev, A., Ozer, Z., Navara, C., Mahajan, S. & Uckun, F.M. Bruton's tyrosine kinase as an inhibitor of the Fas/CD95 death-inducing signaling complex. *J. Biol. Chem.* 274, 1646–1656 (1999).
42. Wang, A.V., Scholl, P.R. & Geha, R.S. Physical and functional association of the high affinity immunoglobulin G receptor (FcγRI) with the kinases Hck and Lyn. *J. Exp. Med.* 180, 1165–1170 (1994).
43. Boyle, K.B. *et al.* Class IA phosphoinositide 3-kinase β and δ regulate neutrophil oxidase activation in response to *Aspergillus fumigatus* hyphae. *J. Immunol.* 186, 2978–2989 (2011).
44. Kawabuchi, M. *et al.* Transmembrane phosphoprotein Cbp regulates the activities of Src-family tyrosine kinases. *Nature* 404, 999–1003 (2000).
45. Saito, K. *et al.* BTK regulates PtdIns-4,5–P2 synthesis: importance for calcium signaling and PI3K activity. *Immunity* 19, 669–678 (2003).
46. Condliffe, A.M. *et al.* Sequential activation of class IB and class IA PI3K is important for the primed respiratory burst of human but not murine neutrophils. *Blood* 106, 1432–1440 (2005).
47. Uckun, F.M. *et al.* Anti-breast cancer activity of LFM-A13, a potent inhibitor of Polo-like kinase (PLK). *Bioorg. Med. Chem.* 15, 800–814 (2007).
48. Mahajan, S. *et al.* Rational design and synthesis of a novel anti-leukemic agent targeting Bruton's tyrosine kinase (BTK), LFM-A13 [alpha-cyano-β-hydroxy-β-methyl-N-(2,5-dibromophenyl)propenamide]. *J. Biol. Chem.* 274, 9587–9599 (1999).

© 2012 Nature America, Inc. All rights reserved.

ONLINE METHODS

Reagents and antibodies. The following reagents were used: lipopolysaccharide derived from *Escherichia coli* or *Pseudomonas aeruginosa*, fMLP, PMA, DHR123, luminol, N-acetyl cysteine, aprotinin, leupeptin, pepstatin and phenylmethyl sulfonyl fluoride (all from Sigma-Aldrich); recombinant human TNF (R&D Systems); Pam$_3$CSK$_4$, LFM-A13, LFM-A11, Syk inhibitor, FAK inhibitor and Ly294002 (all from Calbiochem); and dasatinib, IC87114 and AS-605240 (all from Biovision). Oligodeoxynucleotide CpG-A (5′-GGT GCATCGATGCAGGGGGG-3′) was from Operon Biotechnologies.

The antibodies used were as follows: goat polyclonal antibody to PI(3)K-p85α phosphorylated at Tyr508 (sc-12929), Hck phosphorylated at Tyr411 (sc-12928), rabbit polyclonal antibody to Hck (N-30), anti-PTEN (FL-403), anti-PTP-PEST (H130), anti-FAK (A-17), anti-Vav (C-14), anti-Syk (C-20), anti-SHP2 (C-18) and anti-SHP 1 (C-19), as well as mouse monoclonal antibody (mAb) to p47^{phox} (D-10), p40^{phox} (D-8) or p22^{phox} (CS-9; all from Santa Cruz). Rabbit polyclonal antibody to p101-PI(3)K (07-281) and to gp91^{phox} (07-024) and anti-Rac2 (07-604), biotin-labeled mouse mAb to phosphorylated tyrosine (4G10), as well as horseradish peroxidase-conjugated antibody to goat IgG (AP-180P) were from Upstate; fluorescein isothiocyanate-conjugated mouse mAb to gp91 (7D5) or goat antibody to mouse IgG (238) were from MBL; and mouse mAb to flotillin-1(18), p67^{phox} (29) or PI(3)K-p85 (U15), and fluorescein isothiocyanate-conjugate mouse isotype-matched IgG antibody (MOPC-21) was from BD Pharmingen. Rabbit polyclonal antibody to PI(3)K-p85 (4292), to Lyn (2732), to Lyn phosphorylated at Tyr507 (2731), to Syk phosphorylated Tyr525-Tyr526 (2711), to Src phosphorylated Tyr416 (2101), to FAK phosphorylated Tyr525-Tyr577 (3281), to p40^{phox} phosphorylated at Thr154 (4311) and to caspase-3 (9662), as well as mouse mAb to proliferating cell nuclear antigen (PC-19), were from Cell Signaling. Rabbit mAb to SOD1 (ep1727y), Mal (ep1231y) and catalase (ep1929), as well as rabbit polyclonal antibody to SOD2 (NB100-1992) and to Yes (NBP1-85369), were from Novus Biologicals. Rabbit polyclonal antibody to Bmx (ab73887), to Bmx phosphorylated at Tyr566 (ab59409), to Lyn phosphorylated at Tyr396 (EP503Y), to Vav phosphorylated at Tyr160 (ab4763) and to Prx1 (ab15571), and mouse mAb to Prx2 (12B1), as well as rabbit mAb to Btk (Y440), to CSK (CSK-04), to SHIP (EP378Y) and to Tec (Y398), were from Abcam. Rat mAb to Mal (TIRAP; sebi-1) was from ENZO Life Sciences. Goat polyclonal antibody to CBP (LS-C14699) was from LIFESPAN; anti-β-actin (Ab1) was from Calbiochem; and horseradish peroxidase-conjugated antibody to mouse IgG (NA931), to rabbit IgG (NA934) or to rat IgG (NA9350) was from GE Healthcare. Alexa Flour 546-anti-rabbit IgG (A11035), Alexa Flour 680-anti-rabbit IgG (A10043), Alexa Flour 594-anti-rat IgG (A21209) and Alexa Flour 488-anti-mouse IgG (A21202) were from Invitrogen. Mouse IgG (015-000-003) and rabbit IgG (011-00000-3) were from Jackson ImmunoResearch. Rat IgG2a (eBR2a) was from eBioscience. Horseradish peroxidase-conjugated streptavidin was from Cell Signaling.

The 482H mAb to Btk has been described[49]. Polyclonal antibody to human Btk was raised in rabbits with a Btk peptide of amino acids 169–187 (ENRNGSLKPGSSHRKTKKPC) conjugated to ovalbumin. The antibody collected was further affinity-purified with that same Btk peptide conjugated to thiol-Sepharose 4B (Pharmacia) and was used for immunoprecipitation in some experiments. The specificity of the antibody was confirmed by immunoblot analysis of lysates of Btk-deficient mononuclear cells. Antibody to phosphorylated Ser345 was generated in rabbits by injection of ovalbumin conjugated to a peptide of p47^{phox} phosphorylated at Ser345 (QARPGPQSpPGSPLEEE, where 'Sp' indicates phosphorylated Ser345 (p-Ser345-pep)). The antibody raised was positively affinity-purified with activated thiol-Sepharose 4B adsorbed with p-Ser345-pep. The antibody was further purified by elimination of the fraction that bound to the same peptide of p47^{phox} without phosphorylation at Ser345 (QARPGPQSPGSPLEEE (Ser345-pep)) by passage through thiol-Sepharose 4B conjugated to Ser345-pep; then, the antibody was used for immunoblot analysis. The specificity of the antibody was confirmed by direct enzyme-linked immunosorbent assay with plates coated with Ser345-pep or p-Ser345-pep and by immunoblot analysis experiments showing blockade of the p-p47^{phox} signal by p-Ser345pep but not by Ser345-pep.

Subjects. Patients with XLA (*n* = 17) with stable health were studied (ages and Btk mutations, **Supplementary Fig. 3**). Healthy volunteers (*n* = 18) and patients with CVID (*n* = 5) were enrolled as healthy controls and disease control, respectively. Written informed consent was obtained from all subjects (or their parents). The study protocol was approved by the ethics committee of the Faculty of Medicine, Tokyo Medical and Dental University.

Isolation of neutrophils, monocytes and lymphocytes. Neutrophils were purified from heparinized peripheral blood by a standard technique. All samples were processed within 12 h of blood collection. Peripheral blood diluted in PBS was layered onto a MonoPoly mixture (Flow Laboratories) and centrifuged at 400*g* for 20 min. Layers with enrichment for neutrophils were collected and further purified to a purity of >97% by immunomagnetic negative selection (StemCell Technologies). Sterile and endotoxin-free conditions were used for all procedures. Monocytes were purified from the mononuclear cell–rich fraction with a human monocyte enrichment kit (StemCell Technologies), and lymphocytes were prepared as described[50].

Measurement of production of ROS. Purified neutrophils were loaded for 5 min at 37 °C with DHR123 (5 µg/ml). Cells were washed and then stimulated for 30 min at 37 °C with PMA (100 ng/ml), and the production of ROS was quantified via flow cytometry by measurement of intracellular rhodamine (FACSCalibur; Becton Dickinson). DHR123-loaded neutrophils were also stimulated for 60 min at 37 °C with a TLR ligand (lipopolysaccharide from *E. coli* or *P. aeruginosa*; 100 ng/ml), CpG-A (100 ng/ml) or TNF (1 µg/ml). After incubation, treated and untreated neutrophils were incubated for 5 min at 37 °C with or without fMLP (1 µM), followed by flow cytometry. Results are presented as MFI of treated cells – MFI of untreated cells.

Production of ROS was quantified by standard chemiluminescence. Neutrophils (1.0 × 10^6) were suspended in 0.5 ml PBS containing luminol (10 µM) preheated to 37 °C. After a baseline measurement was obtained, cells were stimulated with a TLR agonist and then with fMLP (1 µM) or with PMA (100 ng/ml); luminescence signals were monitored throughout the reaction.

Detection of apoptosis. Apoptotic cells were identified by staining with annexin V–fluorescein isothiocyanate and 7-AAD (7-amino-actinomycin D; BD Biosciences). Apoptosis was also identified by immunoblot analysis through the detection of cleaved caspase-3 or degraded proliferating cell nuclear antigen.

Flow cytometry. A FACSCalibur (Beckton Dickenson) was used for all flow cytometry analyzing surface expression of gp91, DHR123 staining, annexin V–7-AAD staining, and JC-1 mitochondrial membrane detection as described[50]. All analyses were undertaken after calibration of the fluorescence intensity with CaliBRITE Beads (BD Biosciences).

Subcellular fractionation of neutrophils. Isolated neutrophils were resuspended at a density of 5 × 10^7 cells per ml in ice-cold sonication buffer (HEPES (10 mM), pH 7.2, sucrose (0.15 M), EGTA (1 mM), EDTA (1 mM), NaF (25 mM), leupeptin (10 µg/ml), pepstatin (10 µg/ml), aprotinin (1 µg/ml) and PMSF (1 mM)). After sonication and pelleting on ice, 200 µl supernatant was layered on a discontinuous sucrose gradient consisting of 200 µl of 52% (wt/vol) sucrose, 200 µl of 40% (wt/vol) sucrose and 200 µl of 15% (wt/vol) sucrose. After centrifugation (100,000*g* for 60 min), 160 µl supernatant (cytosol source) and 120 µl interface of the 15%–40% sucrose layers (plasma-membrane source) were collected.

Immunoprecipitation and immunoblot analysis. Lysates were prepared from monocytes and lymphocytes as described[51]. For the preparation of lysates from neutrophils, cells were resuspended in lysis buffer (Tris-HCl (50 mM), pH 7.5, NaCl (150 mM), sucrose (0.25 M), EGTA (5 mM), EDTA (5 mM), leupeptin (15 µg/ml), pepstatin (10 µg/ml), aprotinin (10 µg/ml), PMSF (2.5 mM), 1.0% Nonidet-P40, 0.25% sodium deoxycholate, sodium pyrophosphate (10 mM), NaF (25 mM), Na$_3$VO$_4$ (5 mM), β-glycerophosphate (25 mM) and DNase I (1 µg/ml)), incubated for 30 min on ice and centrifuged at 15,000*g* for 30 min at 4 °C, then supernatants were collected. For extraction of the membrane-raft fraction, 1% n-dodecyl-β-D-maltoside was added to the lysis buffer. Immunoprecipitation and immunoblot analysis were done as described[52]. For immunoprecipitation of cytosolic proteins from neutrophils, cytosolic proteins obtained as described above were diluted in four volumes of immunoprecipitation buffer (Tris-HCl (20 mM), pH 7.5, NaCl (150 mM), sucrose (0.25 M), EGTA (5 mM), EDTA (5 mM), leupeptin (15 µg/ml), pepstatin (10 µg/ml), aprotinin (10 µg/ml), PMSF (2.5 mM), 0.5% Triton-X, sodium pyrophosphate (10 mM), NaF (25 mM), Na$_3$VO$_4$ (5 mM), β-glycerophosphate (50 mM) and levamisole (1 mM)); supernatants were used for immunoprecipitation.

Measurement of phosphatidylinositol-(3,4,5)-trisphosphate. Phosphatidylinositol-(3,4,5)-trisphosphate in unstimulated neutrophils prepared from healthy controls and patients with XLA was measured with an enzyme-linked immunosorbent assay kit in accordance with the manufacturer's instructions (K-2500; Echelon).

Immunofluorescence staining. Cytospin preparations of neutrophils were air-dried and fixed for 10 min with paraformaldehyde in PBS, pH 7.4, then were made permeable for 20 min at −20 °C with acetone, washed, and incubated with the appropriate antibodies. After labeling and washing with 0.2% BSA in PBS, coverslips were mounted with Fluoromount G and the prepared specimens. Nuclei were counterstained with DAPI (4,6-diamidino-2-phenylindole). Slides were analyzed with a fluorescence microscope (FV10i; Olympus) equipped with Fluoview viewer and review station (Olympus). At least 100 cells were inspected for each slide.

Generation of Hph-1-Btk, Hph-1-Btk mutants, and transduction of recombinant protein into cells. Hph-1-tagged Btk constructs were generated by amplification of a full-length Btk cDNA fragment with the appropriate primers (**Supplementary Table 1a**). After the sequence of each PCR product was verified by DNA sequencing, the fragment was ligated into sites of a pET28b vector (Merck) cleaved by *Xma1* and *Sal1*; the vector has a six-histidine site for protein purification and two tandem Hph-1 sequences for protein transduction. Constructs with deletion of the Tec homology domain, SH3 domain or SH2 domain were generated by mutagenesis with the QuikChange SiteDirected Mutagenesis Kit (Stratagene) and the appropriate primers (**Supplementary Table 1b**). The Hph-1-Gal4 construct has been described[52]. Proteins were induced in BL21 Star competent cells (Novagen) as described[52]. Proteins were treated with Detoxi-Gel Endotoxin Removing Gel (Takara Bio) for elimination of endotoxins and were frozen at −80 °C until further use. Neutrophils (1 × 10^6 per ml) were incubated for 1 h with 1 µM Hph-1–tagged proteins (80 µg recombinant Hph-1–tagged full-length-Btk was used for 1 × 10^6 neutrophils for transduction at a concentration of 1 µM) and washed, then ROS production was assayed.

Btk-precipitation assay. Lysates of neutrophils from healthy controls were prepared on ice for 30 min with immunoprecipitation lysis buffer. Supernatants were then treated with protein G beads (GE Health Care) for removal of immunoglobulin G from the neutrophil lysate. For the Btk-precipitation assay, purified Btk recombinant proteins or control recombinant protein were eluted and proteins were measured by BCA protein assay (Pierce). Bacterial supernatants were bound to nickel–nitrilotriacetic acid Sepharose beads (Qiagen) and bound recombinant proteins were eluted, then equimolar amounts of recombinant proteins were rebound to the nickel beads; afterward, samples were washed and then incubated overnight at 4 °C with the cell lysates. Beads were washed four times with lysis buffer and assessed by immunoblot analysis with anti-Mal. Before incubation with cell lysates, the amount of the recombinant protein rebound to nickel beads was assessed by immunoblot analysis with anti-histidine, and the 'dose' was readjusted for further precipitation assays.

Statistical analysis. Student's *t*-test was used for statistical analysis. The software GraphPad Prism 4 was used for these analyses.

49. Futatani, T. *et al.* Deficient expression of Bruton's tyrosine kinase in monocytes from X-linked agammaglobulinemia as evaluated by a flow cytometric analysis and its clinical application to carrier detection. *Blood* **91**, 595–602 (1998).
50. Takahashi, N. *et al.* Impaired CD4 and CD8 effector function and decreased memory T cell populations in ICOS-deficient patients. *J. Immunol.* **182**, 5515–5527 (2009).
51. Morio, T. *et al.* Ku in the cytoplasm associates with CD40 in human B cells and translocates into the nucleus following incubation with IL-4 and anti-CD40 mAb. *Immunity* **11**, 339–348 (1999).
52. Choi, J.M. *et al.* Intranasal delivery of the cytoplasmic domain of CTLA-4 using a novel protein transduction domain prevents allergic inflammation. *Nat. Med.* **12**, 574–579 (2006).

- 155 -

Inherited bone marrow failure syndromes in 2012

Hirotoshi Sakaguchi · Koji Nakanishi ·
Seiji Kojima

Abstract Inherited bone marrow failure syndromes
(CBMFS) are a heterogeneous group of genetic disorders
characterized by bone marrow failure, congenital anoma-
lies, and an increased risk of malignant disease. The rep-
resentative diseases with trilineage involvement are
Fanconi anemia and dyskeratosis congenita, while the
disease with the single lineage cytopenia is Diamond–
Blackfan anemia. Recent advances in our understanding of
these diseases have come from the identification of genetic
lesions responsible for the disease and their pathways.
Although recent studies have identified many causative
genes, mutations of these genes have only been found in
less than half of the patients. Next-generation sequencing
technologies may reveal new causative genes in these
patients. Also, induced pluripotent stem cells derived from
patients with CBMFS will be useful to study the patho-
physiology of the diseases. The only long-term curative
treatment for bone marrow failure in patients with inherited
bone marrow failure syndromes is allogeneic hematopoi-
etic stem cell transplantation, although this procedure has a
risk of severe adverse effects. Multicenter prospective
studies are warranted to establish appropriate conditioning
regimens aimed at reducing transplant-related mortality.

Keywords Inherited bone marrow failure syndrome ·
Fanconi anemia · Diamond–Blackfan anemia ·
Dyskeratosis congenita

H. Sakaguchi · K. Nakanishi · S. Kojima (✉)
Department of Pediatrics,
Nagoya University Graduate School of Medicine,
65 Tsurumai-cho, Showa-ku, Nagoya 466-8550, Japan
e-mail: kojimas@med.nagoya-u.ac.jp

Introduction

Inherited bone marrow failure syndromes (IBMFS) are a
heterogeneous group of genetic disorders characterized by
bone marrow failure, congenital anomalies, and increased
risk of malignant disease. Such bone marrow failure may
affect all three hematopoietic cell lineages or single cell
lineages individually. Diseases characterized by trilineage
involvement include Fanconi anemia and dyskeratosis
congenita, while Diamond–Blackfan anemia results in
single-lineage cytopenia. Recent advances in our under-
standing of these diseases have arisen from the identifica-
tion of genetic lesions responsible for such diseases and
their pathogenic pathways. These investigations have fur-
ther clarified both normal and pathological hematopoiesis.
In this current review, we describe recent insights into
three IBMFS: Fanconi anemia, Diamond–Blackfan anemia,
and dyskeratosis congenita.

Fanconi anemia

Fanconi anemia (FA) is a rare autosomal recessive disease
characterized by congenital abnormalities, progressive
bone marrow failure, and cancer susceptibility. FA, which
has an incidence of less than 10 per million live births, is
the most frequent inherited cause of aplastic anemia [1].
FA is a genetically heterogeneous disease defined by
complementation groups. To date, 15 genes have been
identified as playing a causative in FA and these genes,
FANCA to FANCP, have been cloned [2]. Children with
FA often develop aplastic anemia during the first decade of
life, with death often resulting from complications of bone
marrow failure, such as severe infection or bleeding. FA

patients also develop clonal chromosomal abnormalities in
bone-marrow progenitor cells, such as monosomy 7, which
are associated with myelodysplastic syndrome (MDS) and
acute myeloblastic leukemia (AML) [3]. The gene
FANCD1, which is responsible for complementation group
FA-D1, is identical to the hereditary breast cancer sus-
ceptibility gene, BRCA2, and has been reported as affected
in 3 % of patients with Fanconi anemia. As compared with
children from other FA groups, more severe phenotypes are
seen in FA-D1 patients, such as co-occurrence of multiple
anomalies, development of multiple malignancies with
earlier onset, and increased incidence of leukemia and solid
tumors [4], including Wilms tumor, neuroblastoma, and
brain tumors.

While the treatment of choice for FA patients remains
allogeneic stem cell transplantation (SCT) from an HLA-
matched sibling or unrelated donor, older patients may
develop squamous-cell carcinomas (SCCs) of the head and
neck or gynecological system. In particular, some studies
have demonstrated there is a high incidence of SCC, such
as esophageal cancer, in FA patients who have received
SCT. The age-specific hazard of SCC has been shown to be
4.4-fold higher in patients who receive transplants and, in
addition, SCCs occurred at significantly younger ages in
the transplant group [5]. Thus, further investigations of the
complete care of FA patients need to be undertaken.

Complementation groups and genes of FA

Since cells derived from FA patients are hypersensitive to
DNA interstrand cross-linking (ICL) agents, such as diep-
oxybutane (DEB), mitomycin C (MMC), and cisplatin, it is
expected that FA genes are involved in ICL repair. In 1993,
FANCC was the first FA gene to be cloned by expression
cloning [6, 7]. Subsequently, 15 other genes have been
cloned (Table 1). At present, the FANC genes, which range
from FANC"A" to FANC"P", and the FA pathway have
been shown to resolve ICLs encountered during DNA
replication. There are three primary groups of FA proteins,
which include the FA core complex, the ID (FANCD2/I)
complex, and the BRCA complex (Fig. 1). In these groups,
there are eight FA proteins (FANCA/B/C/E/F/G/L/M) that
form a multi-subunit ubiquitin E3 ligase complex, the FA
core complex, which activates the monoubiquitination of
the ID complex after genotoxic stress, such as ICL, or
during the S phase (Fig. 1) [8, 9]. The monoubiquitinated
ID complex forms foci on damaged DNA. FANCM is also
a crucial gene, as it is a sensor for detecting stalled DNA
replication. The BRCA complex, which is also referred to
as homologous recombination (HR), consists of FANCD1,
FANCJ, FANCN, and FANCO, and is located downstream
of the DI complex on the ICL repair pathway.

Table 1 Genes mutated in patients with Fanconi anemia

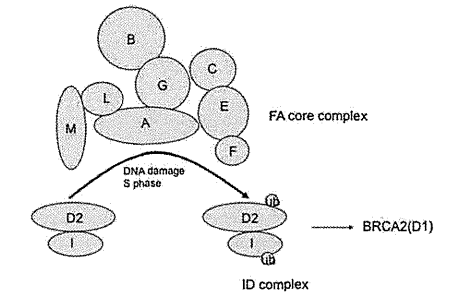|	Other names	Chromosomal Locus	Population in FA patients (%)
FANCA		16q24.3	60–70
FANCB		Xp22.2	2
FANCC		9q22.3	14
FANCD1	BRCA2	13q13.1	3
FANCD2		3p25.3	3
FANCE		6p22-p21	3
FANCF		11p15	2
FANCG		9p13	10
FANCI		15q25-q26	1
FANCJ	BACH1/BRIP1	17q22	2
FANCL		2p16.1	0.20
FANCM		14q21.3	0.20
FANCN	PALB2	16p12.3-p12.2	0.70
FANCO	RAD51C	17q22	0.20
FANCP	SLX4	16p13.3	0.20

Fig. 1 Simplified scheme of the FA pathway. Depending on the FA
core complex, FANCD2 and FANCI are monoubiquitinated after
DNA damage or during the S-phase

Prognosis factors in FA patients

Although FANC gene knockout mice models have been
established, they differ from the hematological phenotypes
of human FA patients [10]. With the exception of the lethal
phenotype of the BRCA2/FANCD1 knockout mouse, the
hematological parameters of the other FA groups show
only a slightly decreased platelet count and a slightly
increased erythrocyte mean cell volume in mice at a young
age, which did not progress to aplastic anemia or leukemia.
However, both male and female mice showed hypogo-
nadism and impaired fertility, which is consistent with the
human FA patient phenotypes.

- 156 -

Recent studies have revealed a relationship between the acetaldehyde and FA pathways. Acetaldehyde is an organic chemical compound that is naturally present in coffee, bread, and ripe fruit, which is produced as product of a plant's normal metabolism. It is also produced by the oxidation of ethylene. In the liver, the enzyme alcohol dehydrogenase (ADH) oxidizes ethanol into acetaldehyde, which is then further oxidized into harmless acetic acid by acetaldehyde dehydrogenase (ALDH). These oxidation reactions are coupled with the reduction of NAD^+ to NADH. ALDH2, an isozyme of ALDH, contains the functional polymorphism, *ALDH2* Glu487Lys. An association between this polymorphism and squamous cell carcinomas, such as esophageal cancer in alcoholics, has been reported. A recent study reported that exposure of cells to acetaldehyde results in a concentration-dependent increase in FANCD2 monoubiquitination [11]. Acetaldehyde also stimulates BRCA1 phosphorylation at Ser1524 and increases the level of H2AX, a marker of homologous recombination. Both modifications occur in a dose-dependent manner.

Another report showed that ALDH2 is essential for the development of FANCD 2(−/−) embryos [12]. Nevertheless, mothers with AA enzyme (ALDH 2(+/−)) can support the development of double-mutant (ALDH2 (−/−)FANCD2(−/−)) mice. These embryos are unusually sensitive to ethanol exposure in utero, with ethanol consumption by postnatal double-deficient mice rapidly precipitating bone marrow failure. ALDH2 (−/−)FANCD2(−/−) mice also spontaneously develop acute leukemia.

This previous study also provided the first evidence of the factors responsible for driving the FA hematological phenotype in mice. DNA damage caused by acetaldehyde may contribute critically to the genesis of fetal alcohol syndrome in fetuses, as well as to abnormal development, bone marrow failure, and cancer predisposition in FA patients. This research group also focused on hematopoietic stem cells (HSCs) in another study [13]. They reported finding that some aged ALDH2(−/−)FANCD2(−/−) mutant mice that did not develop leukemia spontaneously developed aplastic anemia, with a concomitant accumulation of damaged DNA within the hematopoietic stem and progenitor cell (HSPC) pool. Only HSPCs and not the more mature blood precursors require Aldh2 for protection against acetaldehyde toxicity. There is more than a 600-fold reduction in the HSC pool of mice deficient in both FA pathway-mediated DNA repair and acetaldehyde detoxification. This study data indicated that the emergence of bone marrow failure in FA was probably due to aldehyde-mediated genotoxicity restricted to the HSPC pool.

All of the ALDH data suggest that ALDH2 polymorphism is critical to the prognosis of FA patients.

Intercrosslink repair

DNA ICLs are toxic to dividing cells, as they induce mutations, chromosomal rearrangements, and cell death. In order to survive, organisms have developed strategies for dealing with DNA damage. As such, specialized repair pathways have evolved for specific kinds of DNA damage, including double-strand break (DSB) and ICL. Inducers of ICLs are important drugs in cancer treatment and include the well-known chemotherapeutic agents mitomycin C, cisplatin, cyclophosphamide, and their respective derivatives. While cells derived from most individuals with FA are hypersensitive to ICLs, they are generally not hypersensitive to inducers of DSBs such as ionizing radiation, indicating that the ICL repair pathway is distinct from that of DSB.

Homologous recombination is a DNA repair pathway that utilizes strand exchange in a gene conversion reaction involving a single-strand and a DNA duplex. In mammalian cells, this is a major repair pathway for DNA damage such as DSBs. The strand exchange protein RAD51 and the products of the hereditary breast cancer susceptibility genes BRCA1 and BRCA2 [14, 15] are critical proteins in HR in mammalian cells.

In 2005, a cellular study in humans showed that mutation of either the FA core complex members or the FANCD2 monoubiquitination site resulted in HR defects [16]. These defects, however, are mild compared with those resulting from a BRCA2 deficiency. HR measurements in these previous studies were performed with the widely used DR-GFP reporter system, in which a DSB formed by I-SceI endonuclease results in green fluorescent protein-expressing (GFP+) cells repaired by HR (Fig. 2). Further studies have reported on the mechanisms of ICL repair, particularly in terms of the replication-coupled manner. A 2008 study using a cell-free system based on *Xenopus* egg extracts found that ICL is repaired in a replication-dependent manner [17]. Another study in the *Xenopus* egg showed that ubiquitinated FANCI-FANCD2 is essential for replication-dependent ICL repair and that it is able to control the incision step [18]. Development and use of a TR-GFP assay, a modified version of the DR-GFP HR assay system, demonstrated that ICL repair in mammalian cells is dependent on DNA replication. The TR-GFP assay uses a DNA template with a site-specific ICL at sequences that are complemented to triplex-forming oligonucleotide conjugated with psoralen (pso-TFO) [19]. The construct also contains an origin of replication from the Epstein–Barr virus (EBV), enabling replication in human cells. Their results showed that ICL-induced HR was substantially compromised in the absence of FA proteins, suggesting that the FA pathway is specifically involved in replication-coupled HR repair. Use of direct assays for ICL-induced HR in vivo, along with studies that
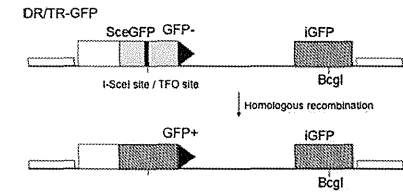
DR/TR-GFP

Fig. 2 DR-GFP assay. In the *DR-GFP* substrate, an I-SceI site is inserted into the GFP gene on sceGFP. GFP is inactivated by the stop-codon in the I-SceI site. To restore functionality of the *GFP* gene, the *iGFP* gene has .8 kb of sequence homology to direct the repair of an I-*Sce*I-cleaved *SceGFP* gene

have demonstrated the involvement of the FA pathway overall, may facilitate delineation of the mechanisms and factors involved in this process.

Diamond–Blackfan anemia

Diamond–Blackfan anemia (DBA) is a rare congenital bone marrow failure syndrome characterized by severe normochromic macrocytic anemia and reticulocytopenia, with selective hypoplasia of erythroid precursors in the bone marrow. Up to 50 % of affected individuals have physical abnormalities including short stature, craniofacial dysmorphism, heart defects, and anomalies of the thumbs and genitourinary tract [20]. Increased risk of malignant disease, such as acute myeloid leukemia and osteogenic sarcoma, has also been reported to occur in this syndrome [21]. The incidence of DBA has been estimated to be 5–7 per million live births in Europe and North America. In a national study conducted in Japan between 2006 and 2010, 65 new DBA patients were registered. During this study period, the mean number of live births per year in Japan was reported to be 1.08 million, putting the incidence of DBA at 12 per each million live births, as most of these patients were diagnosed as DBA during infancy. The majority of these patients are sporadic, with the percentages of patients with autosomal dominant inheritance reported to be less than 10 %. Corticosteroids are recommended as a first line therapy, as these have been reported to improve erythropoiesis in approximately 80 % of DBA patients. In patients refractory to corticosteroids or who develop other forms of cytopenia, HSC transplantation has been suggested as a viable alternative [22].

Molecular pathogenesis

The first DBA gene (RPS19) was identified in 1999 and was found in approximately 25 % of the probands in

western countries [23]. Since then, a total of nine genes encoding large (RPL) or small (RPS) ribosomal subunit proteins were found to be mutated in DBA patients, including RPL5 (6.6 %), RPL11 (4.8 %), RPL35A (3 %), RPS24 (2 %), RPS17 (1 %), RPS7 (1 %), RPS10 (6.4 %), and RPS26 (2.6 %) [24] (Table 2). Collectively, mutations in at least one of these nine genes have been detected in approximately 50–60 % of DBA patients. Of 68 Japanese been examined, mutations in RPS 19, RPL5, RPL11, RPS17, RPS26 were identified in 10 (14.7 %), six (8.8 %), three (4.4 %), one (1.5 %), one (1.5 %), and one (1.5 %), respectively. These mutations have subsequently been determined to occur in 32.4 % of Japanese patients [25, 26]. A low incidence of mutations in the RPS19 gene may account for the overall lower incidence of total mutations in the Japanese population.

As conventional gene sequencing cannot identify large gene deletions, there have been only a few reports of patients with allelic losses in the RPS19 and RPL35A genes. Kuramitsu et al. [26] investigated large deletions of the RP genes using gene copy number variation analysis based on a quantitative-PCR and a single-nucleotide polymorphism (SNP) array. This study used sequencing to screen for large gene deletion in 27 patients without gene mutations. The PCR-based gene copy number assay identified a large deletion in seven (25.9 %) of 27 patients. Of these, three patients had RPS17, two had RPS19, one had RPL5, while one had RPL35A deletions. The SNP array confirmed six of the seven large deletions. Based on these new methods, the frequency of RP gene abnormalities in the DBA patients increased to 42.6 %. All patients with large deletions in DBA genes exhibited malformation with growth retardation. However, half of the patients with a mutation due to sequencing had growth retardation, while all seven patients with a large deletion exhibited growth retardation. While four of seven patients responded to corticosteroids, there were no phenotypic

Table 2 Ribosomal protein gene mutations and deletions in 68 Japanese patients with Diamond–Blackfan anemia

Gene	Mutation	Deletion	Total (%)
RPS 19	10	2	12 (17.6 %)
RPL 5	6	1	7 (10.3 %)
RPS 17	3	0	3 (4.4 %)
RPL 11	3	1	4 (5.9 %)
RPS 10	1	0	1 (1.5 %)
RPS 26	1	0	1 (1.5 %)
RPS 35A	0	1	1 (1.5 %)
RPS 24	0	0	0
RPS 14	0	0	0
Total	22	7	29 (42.6 %)

differences noted between patients with and without large deletions, including response rate to corticosteroids and other malformations.

Farrar et al. [27] also identified RP gene deletions in nine (17 %) of 51 patients without any identifiable mutation by SNP array. Of these nine patients, three had RPS17, two had RPS26, two had RPS19, and two had RPL35A deletions. Clinically, five of the nine patients responded to corticosteroids. Two exhibited short stature. These two studies suggested that genomic deletions may be detected in 4–10 % of DBA patients, which is more common than has been previously suspected. Thus, in addition to conventional gene sequencing, molecular studies of suspected DBA cases should also include either a SNP array or PCR-based gene copy number assay.

Despite extensive sequencing of all the RP genes, at present mutations have only been found in approximately half of DBA patients examined, which raises the question whether other genes are responsible for DBA. Recent advance in genomic sequencing have made it possible to search for new candidate genes. Sankaran et al. [28] performed exome sequencing on two siblings without RP gene mutations. Both affected siblings satisfied the diagnostic criteria for DBA and both parents had normal blood values, suggesting X-linked or autosomal recessive inheritance. During sequencing, at least 10-fold coverage was obtained in more than 93 % of the target bases. After filtering, a total of 74 variants were identified as being shared by the three affected siblings. Of these 74 mutations, 31 were found in two affected siblings but not in the unaffected sibling. No variants were identified that would fit an autosomal recessive model of inheritance. Only the GATA1 gene showed appropriate segregation for an X-linked disease with full penetrance. The mutation in the GATA1 gene is a G-C transversion at position 48,649,736 on the X chromosome and results in a substitution of leucine for valine at amino acid 74 of the GATA1 protein. This mutation impaired production of the full-length form of the exon 2 protein. After screening 62 additional male DBA patients without known mutations for the GATA1 mutation, the study also identified one patient with a mutation in GATA1 at the exon 2-intron 2 junction. It was predicted that this would result in impaired splicing and a frameshift of the full-length GATA1 open reading frame. Overall, this study has opened new avenues for studying the molecular pathogenesis of DBA.

Role of p53 in the pathophysiology of DBA

Although current evidence suggests that impaired ribosomal biogenesis should affect all blood cell lineages, one question remains as to why it affects only the erythroid progenitors. Several animal models have demonstrated the role of p53 in the pathophysiology of DBA. The RPS19-deficient zebrafish model has been shown to have many features of DBA and is accompanied by the up-regulation of the p53 family [29]. Suppression of p53 in the RPS19-deficient zebrafish alleviated the phenotype and improved survival. RPS19 knockdown mouse fetal liver cells, which were created by retrovirus-infected siRNA, showed reduced proliferation but normal differentiation of erythroid cells and an increased level of p53 and p21 [30]. Dutt et al. [31] have examined the accumulation and activity of p53 in different hematopoietic lineages after a partial knockdown of the RPS19 gene in primary human bone marrow-derived CD34 cells. Their study showed that p53 accumulates selectively in erythroid progenitors, resulting in lineage-specific p53 target gene expression, cell cycle arrest, and apoptosis. While pifithrin-α has been shown to inhibit the activity of p53, nutlin-3 activates p53 through the inhibition of HDM2. In addition, nutlin-3 selectivity impairs erythropoiesis, whereas inhibition of p53 by pifithrin-α rescues the erythroid defect. To directly examine whether p53 accumulation is operative in patients with DBA, bone marrow biopsies from eight patients with DBA were stained with anti-human p53 antibody and shown to have strong nuclear staining in two patients and weak nuclear staining in six patients. The erythroid lineage has a low threshold for the induction of p53, which accounts for the selective impaired erythropoiesis in patients with DBA.

Alternative therapies for DBA

Although approximately 80 % of DBA patients initially respond to corticosteroid, half of the responders are steroid-dependent. Only 20 % of these patients achieve remission. Although historically many alternative drugs have been tried, there has been no agreement on a second-line therapy. L-leucine is an essential amino acid and is known to be an activator of mRNA and stimulate protein synthesis through the mammalian target of rapamycin (mTOR) pathway. L-leucine treatment of the RPS19-deficient zebrafish model results in a striking improvement of anemia and developmental defects. These findings were reproduced in primary human CD34 cells after knockdown of the RPS19 gene [32]. Therapeutic effect of L-leucine has also been confirmed in the mouse model for RPS19-deficient DBA and shown to be associated with reduced p53 activity in hematopoietic progenitors [33]. Recently, leucine has been used on an investigational basis in one patient with DBA and is reported to have achieved a remission [34].

These findings support commencement of a clinical trial with L-leucine as an alternative therapy for DBA.

Dyskeratosis congenita

Clinical features of patients with dyskeratosis congenita

Dyskeratosis congenita (DC) is a rare inherited disease characterized by the classical mucocutaneous triad of abnormal skin pigmentation, nail dystrophy, and mucosal leucoplakia in approximately 80–90 % of patients [34]. Patients with DC are unable to maintain the telomere complex that protects the chromosome ends and consequently have very short telomeres [35]. Shortened telomeres can cause a wide variety of clinical features across a phenotypic spectrum consisting not only of mucocutaneous abnormalities but also multisystem symptoms including bone marrow failure, pulmonary fibrosis, hepatic fibrosis, and predisposition to malignancy [36, 37]. Indeed, non-mucocutaneous features, such as bone marrow failure and pulmonary fibrosis, occasionally precede mucocutaneous abnormalities, making it difficult to diagnose patients with DC based on clinical features alone. The incidence of DC is estimated to be one per million live births.

The diagnostic criteria for DC proposed by Vulliamy [38] include one or more of the three classic mucocutaneous features combined with hypoplastic bone marrow and at least two other somatic features known to occur in DC. The primary causes of mortality in patients with DC are bone marrow failure syndrome (60–70 %), pulmonary complications (10–15 %), and malignancy (particularly MDS and AML) (10 %) [36, 37].

Genetic background of DC

DC is a genetically heterogeneous disorder, showing autosomal recessive, autosomal dominant, and X-linked inheritance. The DKC1 gene on chromosome (chr) Xq28, which encodes dyskerin, was the first gene identified in the X-linked DC patients [39]. Dyskerin has a close association with the RNA component of telomerase (TERC), and mutations in dyskerin cause a reduction in accumulation of TERC and reduced telomere length [35]. In addition to its role in the biogenesis of telomerase RNA dyskerin is involved in ribosomal RNA biogenesis. Dyskerin catalyzes uridine to pseudouridine, which is a critical step for ribosomal RNA maturation and function. These findings imply that both telomere and ribosomal defects may occur in patients with DKC1 mutations. Subsequently, heterozygous TERC mutations have also been found in autosomal dominant DC patients [40]. Genetic screening has identified mutations of other components of the telomerase complex, including TERT (chr 5p15) [41, 42], NOP10 (chr 15q14-q15) [43], and NHP2 (chr 5q35) [44] in patients with rare autosomal recessive DC. Mutations of TERT have also been reported in the autosomal dominant family [45].

Moreover, heterozygous mutations of TINF2 (chr 14q12) that encode TIN2, which is the main component of shelterin and which protects telomeres, have been identified in <11 % of DC patients [46, 47].

More recently, mutations of TCAB1 (chr 17p13) were identified in patients with DC as autosomal recessive forms [48]. Venteicher et al. [49] found that TCAB1 associates with TERT, dyskerin and TERC, and small Cajal body RNAs (scaRNAs) that are involved in modifying splicing RNAs to control telomerase trafficking. TCAB1 defects prevented TERC from associating with the Cajal bodies, which disrupted the telomerase–telomere association. A recent case report described biallelic mutations of the CTC1 gene (chr 17p13) in a patient with DC [50]. This gene was originally described as causative gene of the Coats plus syndrome, which is a form of cerebroretinal microangiopathy with calcifications and cysts (CRMCC). The mutation frequencies of these new genes for DC remain unknown.

At present, eight of the mutated genes in DC have been shown to be associated with the telomerase holoenzyme (TERT, TERC, DKC1, NOP10, NHP2, TCAB1, and CTC1) or the shelterin complex (TINF2), accounting for approximately 50 % of DC patients. Mutations in telomerase and telomere components have also been identified in patients with aplastic anemia, pulmonary fibrosis, and liver diseases that did not have any mucocutaneous manifestations [45, 46, 51–59]. These findings suggest that defective telomere maintenance causes not only classical DC, but also a broad spectrum of diseases previously thought to be idiopathic and thus this has led to a new concept of diseases termed "syndromes of telomere shortening".

Cryptic DC patients in aplastic anemia

Patients with DC have been shown to have disease diversity in terms of age at onset, symptoms, and severity. This diversity occurs even among the patients with the same gene mutation. Bone marrow failure sometimes precedes mucocutaneous manifestations in patients with DC, and a substantial proportion of patients with aplastic anemia have shorter telomeres compared with normal individuals [60, 61]. These observations have prompted screening for gene mutations responsible for telomere maintenance in patients with aplastic anemia and other bone marrow failure syndromes. This screening identified mutations in TERC and TERT in 3 % of the aplastic anemia patients [54, 55]. Our research group conducted a study in Japanese children with aplastic anemia and identified two of 96 as having the TERT mutations, although none of the patients had a TERC mutation [53]. Patients with TERC or TERT mutations have been shown to have very short telomeres in their blood cells. Recently, Du et al. [52] found that 6 (5.5 %) of 109

pediatric patients with severe aplastic anemia had mutations of *TINF2*. In an unpublished study, our research group screened for mutations of *TINF2* and found that of the 96 pediatric patients with aplastic anemia that were examined, none exhibited any mutations of this gene.

Three methods are commonly used for measuring telomere length, including Southern blot, real-time polymerase chain reaction, and flow cytometry and fluorescence in situ hybridization (flow-FISH). Of these, the flow-FISH has been shown to be the most appropriate when undertaking "prospective" screening [62, 63]. As shown in Fig. 3, patients with DC and aplastic anemia with the *TERT* mutation were all found to have very short telomeres as compared with the idiopathic aplastic anemia patients and normal individuals. As a small subset of patients with apparently idiopathic aplastic anemia have been shown to carry telomere gene mutations, identification of such patients is critical for informing treatment decisions. Aplastic anemia patients should be routinely screened for telomere gene mutations prior to starting any treatment. However, because screening of gene mutations can be both laborious and time consuming, we have adopted the screening of telomere length in blood cells rather than screening of gene mutations.

It should be noted that short telomeres are not specific for patients with DC, as they are also seen in patients with other bone marrow failure syndromes. Although short telomeres have also been found in patients with other congenital bone marrow failure syndromes, such as Shwachman–Diamond syndrome and Fanconi anemia, telomere lengths in patients with DC have been demonstrated to be
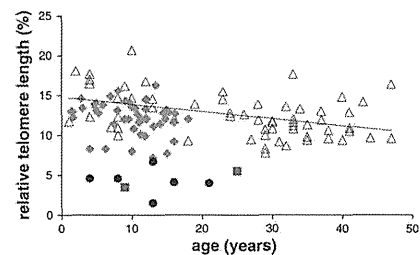

Fig. 3 Relative telomere length in peripheral blood lymphocytes from patients with dyskeratosis congenita (*filled circles*), patients with aplastic anemia harboring TERT mutations (*filled squares*), patients with idiopathic aplastic anemia (*filled argyles*) and normal individuals (*open triangles*). Telomere lengths were measured by flow cytometry-fluorescent in situ hybridization (flow-FISH). Relative telomere length was calculated as the ratio between the telomere signal of each sample and the telomere signal of the control cell line (cell line 1301). These data were provided by the Department of Pediatrics, Nagoya University Graduate School of Medicine

shorter than those in all other bone marrow failure syndromes. In fact, telomere length in most patients with DC is below the first percentile of telomere length found in healthy controls [64].

Family members of patients with DC should receive genetic counseling to rule out if they are silent carriers. In particular, genetic counseling is necessary during the proband search for a donor for HSC transplantation. Studies on telomere length analyses in families with DC have shown that mutated carriers with clinical signs of bone marrow failure have short telomeres. Even so, telomere length cannot predict the presence or absence of a mutation in family members with bone marrow failure. In addition, there have been rare cases that show normal telomere length, even though the subject harbors the same mutation as the proband. This suggests that mutation alone does not sufficiently explain the reduction of telomere length [51].

Clinical management for DC

Bone marrow failure and immune deficiency are the most common causes of death in up to 60–70 % of patients with DC. Androgen (e.g. oxymetholone) has been used to improve cytopenia in patients with DC since the 1960s. However, the mechanism of action of androgen has not been well understood until recently. Calado et al. [65] showed that in vitro exposure of normal peripheral blood cells to androgen produced higher TERT mRNA levels. When these patients were treated with cells from patients who had a heterozygous mutation of the telomerase, it was possible to restore their low baseline telomerase activity to normal levels. Thus, as telomere shortening is closely associated with malignant disease, androgen therapy might be able to prevent or postpone the development of various types of cancers. Erythropoietin and/or G-CSF combined with androgen has occasionally provided transient hematopoietic recovery to poor responders to androgen alone [66]. However, this combination should be used with caution, as severe splenic peliosis and fatal rupture have been reported in two patients with DC who received simultaneous administration of androgen and G-CSF [67].

Allogeneic HSC transplantation is the only curative treatment for bone marrow failure in patients with DC. However, the outcome in previous reports has been disappointing due to unacceptable transplant-related toxicities, including severe pulmonary/liver complications, especially in transplants from an alternative donor [68, 69]. To avoid these complications, non-myeloablative conditioning regimens have been recently used in several cases. Dietz et al. [70] reported encouraging results of six patients with DC who received a fludarabine-based non-myeloablative regimen. Of the four surviving patients, three were recipients of unrelated grafts. Non-myeloablative

transplants are expected to provide improvement in the short-term survival. At our institute, three patients with DC underwent allogeneic bone marrow transplantation following non-myeloablative conditioning from 2003 to 2009. Successful engraftment was achieved in all patients with only a few regimen-related toxicities, and at the present time all continue to survive without any symptoms [71]. However, due the late effects of conditioning agents and allogeneic immune responses within the recipient's organs, such as the lung and liver, longer-term follow-ups are necessary to definitively clarify the present results.

Conclusion

Although recent studies have identified many causative genes, mutations of these genes have only been found in half of the patients with DBA or DKC. Next-generation sequencing (or massive parallel sequencing) technologies have led to a tremendous revolution in genomics, with their effects currently becoming increasingly widespread. This new strategy may soon be able to reveal the remaining unknown causative genes in IBMFS.

Recently, Agarwal et al. [72] established induced pluripotent stem cells (iPSCs) derived from a patient with DC and showed that the reprogrammed DC cells overcame a critical limitation in TERC levels to restore the telomere maintenance and self-renewal. These findings indicate that drugs or gene therapy that upregulate TERC activity may show therapeutic potential in patients with DC. These same strategies may also be applicable for other IBMFS.

The only long-term curative treatment for bone marrow failure in patients with IBMFS is allogeneic HSC transplantation, although this procedure has a risk of severe adverse effects. Multicenter prospective studies are needed to establish appropriate conditioning regimens aimed at reducing transplant-related mortality. Future studies must aim to improve short-term outcomes, such as hematological recovery, and to decrease the incidence of late adverse effects.

References

1. Joenje H, Patel KJ. The emerging genetic and molecular basis of Fanconi anaemia. Nat Rev Genet. 2001;2:446–57.
2. Kim H, D'Andrea AD. Regulation of DNA cross-link repair by the Fanconi anemia/BRCA pathway. Genes Dev. 2012;26:1393–408.
3. D'Andrea AD, Grompe M. The Fanconi anaemia/BRCA pathway. Nat Rev Cancer. 2003;3:23–34.
4. Alter BP, Rosenberg PS, Brody LC. Clinical and molecular features associated with biallelic mutations in FANCD1/BRCA2. J Med Genet. 2007;44:1–9.
5. Rosenberg PS, Socie G, Alter BP, Gluckman E. Risk of head and neck squamous cell cancer and death in patients with Fanconi anemia who did and did not receive transplants. Blood. 2005;105:67–73.
6. Whitney MA, Saito H, Jakobs PM, Gibson RA, Moses RE, Grompe M. A common mutation in the FACC gene causes Fanconi anaemia in Ashkenazi Jews. Nat Genet. 1993;4:202–5.
7. Gibson RA, Hajianpour A, Murer-Orlando M, Buchwald M, Mathew CG. A nonsense mutation and exon skipping in the Fanconi anaemia group C gene. Hum Mol Genet. 1993;2:797–9.
8. Garcia-Higuera I, Taniguchi T, Ganesan S, Meyn MS, Timmers C, Hejna J, et al. Interaction of the Fanconi anemia proteins and BRCA1 in a common pathway. Mol Cell. 2001;7:249–62.
9. Smogorzewska A, Matsuoka S, Vinciguerra P, McDonald ER 3rd, Hurov KE, Luo J, et al. Identification of the FANCI protein, a monoubiquitinated FANCD2 paralog required for DNA repair. Cell. 2007;129:289–301.
10. Carreau M. Not-so-novel phenotypes in the Fanconi anemia group D2 mouse model. Blood. 2004;103:2430.
11. Marietta C, Thompson LH, Lamerdin JE, Brooks PJ. Acetaldehyde stimulates FANCD2 monoubiquitination, H2AX phosphorylation, and BRCA1 phosphorylation in human cells in vitro: implications for alcohol-related carcinogenesis. Mutat Res. 2009;664:77–83.
12. Langevin F, Crossan GP, Rosado IV, Arends MJ, Patel KJ. Fancd2 counteracts the toxic effects of naturally produced aldehydes in mice. Nature. 2011;475:53–8.
13. Garaycoechea JI, Crossan GP, Langevin F, Daly M, Arends MJ, Patel KJ. Genotoxic consequences of endogenous aldehydes on mouse haematopoietic stem cell function. Nature. 2012;489:571–5.
14. Moynahan ME, Chiu JW, Koller BH, Jasin M. Brca1 controls homology-directed DNA repair. Mol Cell. 1999;4:511–8.
15. Moynahan ME, Pierce AJ, Jasin M. BRCA2 is required for homology-directed repair of chromosomal breaks. Mol Cell. 2001;7:263–72.
16. Nakanishi K, Yang YG, Pierce AJ, Taniguchi T, Digweed M, D'Andrea AD, et al. Human Fanconi anemia monoubiquitination pathway promotes homologous DNA repair. Proc Natl Acad Sci USA. 2005;102:1110–5.
17. Raschle M, Knipscheer P, Enoiu M, Angelov T, Sun J, Griffith JD, et al. Mechanism of replication-coupled DNA interstrand crosslink repair. Cell. 2008;134:969–80.
18. Knipscheer P, Raschle M, Smogorzewska A, Enoiu M, Ho TV, Scharer OD, et al. The Fanconi anemia pathway promotes replication-dependent DNA interstrand cross-link repair. Science. 2009;2009(326):1698–701.
19. Nakanishi K, Cavallo F, Perrouault L, Giovannangeli C, Moynahan ME, Barchi M, et al. Homology-directed Fanconi anemia pathway cross-link repair is dependent on DNA replication. Nat Struct Mol Biol. 2011;18:500–3.
20. Alter BP, Young NS. The bone marrow failure syndromes. In: Nathan DG, Orkin HS, editors. Hematology of infancy and childhood, vol 1. Philadelphia: Saunders; 1998. p. 237–335.
21. Vlachos A, Rosenberg PS, Atsidaftos E, Alter BP, Lipton JM. Incidence of neoplasia in Diamond Blackfan anemia: a report from the Diamond Blackfan Anemia Registry. Blood. 2012;119:3815–9.
22. Mugishima H, Ohga S, Ohara A, Kojima S, Fujisawa K, For the Aplastic Anemia Committee of the Japanese Society of Pediatric Hematology. Hematopoietic stem cell transplantation for Diamond–Blackfan anemia: a report from the Aplastic Anemia Committee of the Japanese Society of Pediatric Hematology. Pediatr Transpl. 2007;11:601–7.
23. Draptchinskaia N, Gustavsson P, Andersson B, Pettersson M, Willig TN, Dianzani I, et al. The gene encoding ribosomal

protein S19 is mutated in Diamond–Blackfan anaemia. Nat Genet. 1999;21:169–75.

24. Boria I, Garelli E, Gazda HT, Aspesi A, Quarello P, Pavesi E, et al. The ribosomal basis of Diamond–Blackfan anemia: mutation and database update. Hum Mutat. 2010;31:1269–79.

25. Konno Y, Toki T, Tandai S, Xu G, Wang R, Terui K, et al. Mutations in the ribosomal protein genes in Japanese patients with Diamond–Blackfan anemia. Haematologica. 2010;95:1293–9.

26. Kuramitsu M, Sato-Otsubo A, Morio T, Takagi M, Toki T, Terui K, et al. Extensive gene deletions in Japanese patients with Diamond–Blackfan anemia. Blood. 2012;119:2376–84.

27. Farrar JE, Vlachos A, Atsidaftos E, Carlson-Donohoe H, Markello TC, Arceci RJ, et al. Ribosomal protein gene deletions in Diamond–Blackfan anemia. Blood. 2011;118:6943–51.

28. Sankaran VG, Ghazvinian R, Do R, Thiru P, Vergilio JA, Beggs AH, et al. Exome sequencing identifies GATA1 mutations resulting in Diamond–Blackfan anemia. J Clin Invest. 2012;122:2439–43.

29. Danilova N, Sakamoto KM, Lin S. Ribosomal protein S19 deficiency in zebrafish leads to developmental abnormalities and defective erythropoiesis through activation of p53 protein family. Blood. 2008;112:5228–37.

30. Sieff CA, Yang J, Merida-Long LB, Lodish HF. Pathogenesis of the erythroid failure in Diamond Blackfan anaemia. Br J Haematol. 2010;148:611–22.

31. Dutt S, Narla A, Lin K, Mullally A, Abayasekara N, Megerdichian C, et al. Haploinsufficiency for ribosomal protein genes causes selective activation of p53 in human erythroid progenitor cells. Blood. 2011;117:2567–76.

32. Payne EM, Virgilio M, Narla A, Sun H, Levine M, Paw BH, et al. L-leucine improves the anemia and developmental defects associated with Diamond–Blackfan anemia and del(5q) MDS by activating the mTOR pathway. Blood. 2012;120:2214–24.

33. Jaako P, Debnath S, Olsson K, Bryder D, Flygare J, Karlsson S. Dietary L-leucine improves the anemia in a mouse model for Diamond–Blackfan anemia. Blood. 2012;120:2225–8.

34. Kirwan M, Dokal I. Dyskeratosis congenita, stem cells and telomeres. Biochim Biophys Acta. 2009;1792:371–9.

35. Mitchell JR, Wood E, Collins K. A telomerase component is defective in the human disease dyskeratosis congenita. Nature. 1999;402:551–5.

36. Dokal I. Dyskeratosis congenita in all its forms. Br J Haematol. 2000;110:768–79.

37. Walne AJ, Dokal I. Advances in the understanding of dyskeratosis congenita. Br J Haematol. 2009;145:164–72.

38. Vulliamy TJ, Marrone A, Knight SW, Walne A, Mason PJ, Dokal I. Mutations in dyskeratosis congenita: their impact on telomere length and the diversity of clinical presentation. Blood. 2006;107:2680–5.

39. Heiss NS, Knight SW, Vulliamy TJ, Klauck SM, Wiemann S, Mason PJ, Poustka A, Dokal I. X-linked dyskeratosis congenita is caused by mutations in a highly conserved gene with putative nucleolar functions. Nat Genet. 1998;19:32–8.

40. Vulliamy T, Marrone A, Goldman F, Dearlove A, Bessler M, Mason PJ, et al. The RNA component of telomerase is mutated in autosomal dominant dyskeratosis congenita. Nature. 2001;413:432–5.

41. Armanios M, Chen JL, Chang YP, Brodsky RA, Hawkins A, Griffin CA, et al. Haploinsufficiency of telomerase reverse transcriptase leads to anticipation in autosomal dominant dyskeratosis congenita. Proc Natl Acad Sci USA. 2005;102:15960–4.

42. Marrone A, Walne A, Tamary H, Masunari Y, Kirwan M, Beswick R, et al. Telomerase reverse-transcriptase homozygous mutations in autosomal recessive dyskeratosis congenita and Hoyeraal–Hreidarsson syndrome. Blood. 2007;110:4198–205.

43. Walne AJ, Vulliamy T, Marrone A, Beswick R, Kirwan M, Masunari Y, et al. Genetic heterogeneity in autosomal recessive dyskeratosis congenita with one subtype due to mutations in the telomerase-associated protein NOP10. Hum Mol Genet. 2007;16:1619–29.

44. Vulliamy T, Beswick R, Kirwan M, Marrone A, Digweed M, Walne A, et al. Mutations in the telomerase component NHP2 cause the premature ageing syndrome dyskeratosis congenita. Proc Natl Acad Sci USA. 2008;105:8073–8.

45. Vulliamy TJ, Walne A, Baskaradas A, Mason PJ, Marrone A, Dokal I. Mutations in the reverse transcriptase component of telomerase (TERT) in patients with bone marrow failure. Blood Cells Mol Dis. 2005;34:257–63.

46. Walne AJ, Dokal I. Dyskeratosis congenita: a historical perspective. Mech Ageing Dev. 2008;129:48–59.

47. Savage SA, Giri N, Baerlocher GM, Orr N, Lansdorp PM, Alter BP. TINF2, a component of the shelterin telomere protection complex, is mutated in dyskeratosis congenita. Am J Hum Genet. 2008;82:501–9.

48. Zhong F, Savage SA, Shkreli M, et al. Disruption of telomerase trafficking by TCAB1 mutation causes dyskeratosis congenita. Genes Dev. 2011;25:11–6.

49. Venteicher AS, Abreu EB, Meng Z, McCann KE, Terns RM, Veenstra TD, Terns MP, Artandi SE. A human telomerase holoenzyme protein required for Cajal body localization and telomere synthesis. Science. 2009;323:644–8.

50. Keller RB, Gagne KE, Usmani GN, Asdourian GK, Williams DA, Hofmann I, Agarwal S. CTC1 Mutations in a patient with dyskeratosis congenita. Pediatr Blood Cancer. 2012;59:311–4.

51. Du HY, Pumbo E, Ivanovich J, An P, Maziarz RT, Reiss UM, et al. TERC and TERT gene mutations in patients with bone marrow failure and the significance of telomere length measurements. Blood. 2009;113:309–16.

52. Du HY, Mason PJ, Bessler M, Wilson DB. TINF2 mutations in children with severe aplastic anemia. Pediatr Blood Cancer. 2009;52:687.

53. Liang J, Yagasaki H, Kamachi Y, Hama A, Matsumoto K, Kato K, et al. Mutations in telomerase catalytic protein in Japanese children with aplastic anemia. Haematologica. 2006;91:656–8.

54. Yamaguchi H, Calado RT, Ly H, Kajigaya S, Baerlocher GM, Chanock SJ, et al. Mutations in TERT, the gene for telomerase reverse transcriptase, in aplastic anemia. N Engl J Med. 2005;352:1413–24.

55. Yamaguchi H, Baerlocher GM, Lansdorp PM, Chanock SJ, Nunez O, Sloand E, et al. Mutations of the human telomerase RNA gene (TERC) in aplastic anemia and myelodysplastic syndrome. Blood. 2003;102:916–8.

56. Vulliamy T, Marrone A, Dokal I, Mason PJ. Association between aplastic anaemia and mutations in telomerase RNA. Lancet. 2002;359:2168–70.

57. Tsakiri KD, Cronkhite JT, Kuan PJ, Xing C, Raghu G, Weissler JC, et al. Adult-onset pulmonary fibrosis caused by mutations in telomerase. Proc Natl Acad Sci USA. 2007;104:7552–7.

58. Armanios MY, Chen JJ, Cogan JD, Alder JK, Ingersoll RG, Markin C, et al. Telomerase mutations in families with idiopathic pulmonary fibrosis. N Engl J Med. 2007;356:1317–26.

59. Calado RT, Regal JA, Kleiner DE, Schrump DS, Peterson NR, Pons V, et al. A spectrum of severe familial liver disorders associate with telomerase mutations. PLoS ONE. 2009;4:e7926.

60. Ball SE, Gibson FM, Rizzo S, Tooze JA, Marsh JC, Gordon-Smith EC. Progressive telomere shortening in aplastic anemia. Blood. 1998;91:3582–92.

61. Lee JJ, Kook H, Chung IJ, Na JA, Park MR, Hwang TJ, et al. Telomere length changes in patients with aplastic anaemia. Br J Haematol. 2001;112:1025–30.

62. Baerlocher GM, Vulto I, de Jong G, Lansdorp PM. Flow cytometry and FISH to measure the average length of telomeres (flow FISH). Nat Protoc. 2006;1:2365–76.

63. Canela A, Klatt P, Blasco MA. Telomere length analysis. Methods Mol Biol. 2007;371:45–72.

64. Alter BP, Baerlocher GM, Savage SA, Chanock SJ, Weksler BB, Willner JP, et al. Very short telomere length by flow fluorescence in situ hybridization identifies patients with dyskeratosis congenita. Blood. 2007;110:1439–47.

65. Calado RT, Yewdell WT, Wilkerson KL, Regal JA, Kajigaya S, Stratakis CA, et al. Sex hormones, acting on the TERT gene, increase telomerase activity in human primary hematopoietic cells. Blood. 2009;114:2236–43.

66. Alter BP, Gardner FH, Hall RE. Treatment of dyskeratosis congenita with granulocyte colony-stimulating factor and erythropoietin. Br J Haematol. 1997;97:309–11.

67. Giri N, Pitel PA, Green D, Alter BP. Splenic peliosis and rupture in patients with dyskeratosis congenita on androgens and granulocyte colony-stimulating factor. Br J Haematol. 2007;138:815–7.

68. Alter BP, Giri N, Savage SA, Rosenberg PS. Cancer in dyskeratosis congenita. Blood. 2009;113:6549–57.

69. de la Fuente J, Dokal I. Dyskeratosis congenita: advances in the understanding of the telomerase defect and the role of stem cell transplantation. Pediatr Transpl. 2007;11:584–94.

70. Dietz AC, Orchard PJ, Baker KS, Giller RH, Savage SA, Alter BP, et al. Disease-specific hematopoietic cell transplantation: nonmyeloablative conditioning regimen for dyskeratosis congenita. Bone Marrow Transpl. 2011;46:98–104.

71. Nishio N, Takahashi Y, Ohashi H, Doisaki S, Muramatsu H, Hama A, Shimada A, Yagasaki H, Kojima S. Reduced-intensity conditioning for alternative donor hematopoietic stem cell transplantation in patients with dyskeratosis congenita. Pediatr Transpl. 2011;15:161–6.

72. Agarwal S, Loh YH, McLoughlin EM, Huang J, Park IH, Miller JD, et al. Telomere elongation in induced pluripotent stem cells from dyskeratosis congenita patients. Nature. 2010;464:292–6.

To the editor:

Rabbit antithymocyte globulin and cyclosporine as first-line therapy for children with acquired aplastic anemia

Horse antithymocyte globulin (hATG) and cyclosporine have been used as standard therapy for children with acquired aplastic anemia (AA) for whom an HLA-matched family donor is unavailable. However, in 2009, hATG (lymphoglobulin; Genzyme) was withdrawn and replaced by rabbit ATG (rATG; thymoglobulin; Genzyme) in Japan. Many other countries in Europe and Asia are facing the same situation.[1] Marsh et al recently reported outcomes for 35 adult patients with AA who were treated with rATG and cyclosporine as a first-line therapy.[2] Although the hematologic response rate was 40% at 6 months, several patients subsequently achieved late responses. The best response rate was 60% compared with 67% in a matched-pair control group of 105 patients treated with hATG. The overall and transplantation-free survival rates appeared to be significantly inferior with rATG compared with hATG at 68% versus 86% (P = .009) and 52% versus 76% (P = .002), respectively. These results are comparable to those from a prospective randomized study reported by Scheinberg et al comparing hATG and rATG.[3] Both studies showed the superiority of hATG over rATG.[2,3]

We recently analyzed outcomes for 40 Japanese children (median age, 9 years; range, 1-15) with AA treated using rATG and cyclosporine. The median interval from diagnosis to treatment was 22 days (range, 1-203). The numbers of patients with very severe, severe, and nonsevere disease were 14, 10, and 16, respectively. The ATG dose was 3.5 mg/kg/day for 5 days. The median follow-up time for all patients was 22 months (range, 6-38). At 3 months, no patients had achieved a complete response (CR) and partial response (PR) was seen in only 8 patients (20.0%). At 6 months, the numbers of patients with CR and PR were 2 (5.0%) and 17 (42.5%), respectively. After 6 months, 5 patients with PR at 6 months had achieved CR and 4 patients with no response at 6 months had achieved PR, offering a total best response rate of 57.5%. Two patients relapsed at 16 and 19 months without receiving any second-line treatments. Two patients with no re-

sponse received a second course of rATG at 13 and 17 months, but neither responded. Sixteen patients underwent hematopoietic stem cell transplantation (HSCT) from alternative donors (HLA-matched unrelated donors, n = 13; HLA-mismatched family donors, n = 3). Two deaths occurred after rATG therapy, but no patients died after HSCT. Causes of death were intracranial hemorrhage at 6 months and acute respiratory distress syndrome at 17 months. The overall 2-year survival rate was 93.8% and the 2-year transplantation-free survival rate was 50.3% (Figure 1).

In our previous prospective studies with hATG, the response rates after 6 months were 68% and 70%, respectively, with no increases in response rates observed after 6 months.[4,5] Our results support the notion that rATG is inferior to hATG for the treatment of AA in children. First-line HSCT from an alternative donor may be justified, considering the excellent outcomes in children who received salvage therapies using alternative donor HSCT.

Yoshiyuki Takahashi
Department of Pediatrics, Nagoya Graduate School of Medicine,
Nagoya, Japan

Hideki Muramatsu
Department of Pediatrics, Nagoya Graduate School of Medicine,
Nagoya, Japan

Naoki Sakata
Department of Pediatrics, Kinki University School of Medicine,
Osaka, Japan

Nobuyuki Hyakuna
Center of Bone Marrow Transplantation, Ryukyu University Hospital,
Okinawa, Japan

Kazuko Hamamoto
Department of Pediatrics, Hiroshima Red Cross Hospital,
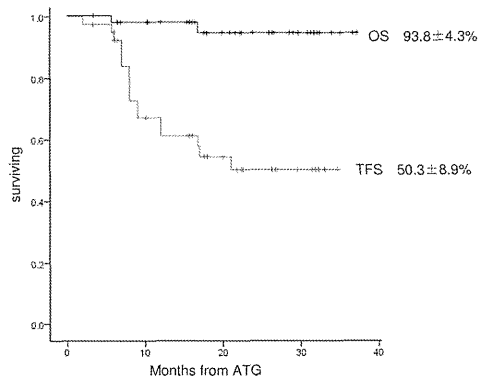*Hiroshima, Japan*

Figure 1. Kaplan-Meier estimates of overall survival (OS) and transplantation-free survival (TFS) in 40 Japanese children with AA. Survival was investigated using Kaplan-Meier methods. OS for all patients with AA after rATG and cyclosporine as first-line therapy included patients who later received HSCT for nonresponse to rATG. In the analysis of TFS for all patients treated with rATG and CSA, transplantation was considered an event.

Ryoji Kobayashi
Department of Pediatrics, Sapporo Hokuyu Hospital,
Sapporo, Japan

Etsuro Ito
Department of Pediatrics, Hirosaki University School of Medicine,
Hirosaki, Japan

Hiroshi Yagasaki
Department of Pediatrics, School of Medicine, Nihon University,
Tokyo, Japan

Akira Ohara
Division of Blood Transfusion, Toho University Omori Hospital,
Tokyo, Japan

Akira Kikuchi
Department of Pediatrics, Teikyo University School of Medicine,
Tokyo, Japan

Akira Morimoto
Department of Pediatrics, Jichi Medical University School of Medicine,
Tochigi, Japan

Hiromasa Yabe
Department of Cell Transplantation and Regenerative Medicine,
Tokai University School of Medicine,
Isehara, Japan

Kazuko Kudo
Division of Hematology and Oncology, Shizuoka Children's Hospital,
Shizuoka, Japan

Ken-ichiro Watanabe
Department of Pediatrics, Graduate School of Medicine, Kyoto University,
Kyoto, Japan

Shouichi Ohga
Department of Perinatal and Pediatric Medicine,
Graduate School of Medical Sciences, Kyushu University,
Fukuoka, Japan

Seiji Kojima
Department of Pediatrics, Nagoya Graduate School of Medicine,
Nagoya, Japan

on behalf of the Japan Childhood Aplastic Anemia Study Group

References

1. Dufour C, Bacigalupo A, Oneto R, et al. Rabbit ATG for aplastic anaemia treatment: a backward step? *Lancet.* 2011;378(9806):1831-1833.
2. Marsh JC, Bacigalupo A, Schrezenmeier H, et al. Prospective study of rabbit antithymocyte globulin and cyclosporine for aplastic anemia from the EBMT Severe Aplastic Anaemia Working Party. *Blood.* 2012;119(23):5391-5396.
3. Scheinberg P, Nunez O, Weinstein B, et al. Horse versus rabbit antithymocyte globulin in acquired aplastic anemia. *N Engl J Med.* 2011;365(5):430-438.
4. Kojima S, Hibi S, Kosaka Y, et al. Immunosuppressive therapy using antithymocyte globulin, cyclosporine, and danazol with or without human granulocyte colony-stimulating factor in children with acquired aplastic anemia. *Blood.* 2000;96(6):2049-2054.
5. Kosaka Y, Yagasaki H, Sano K, et al. Prospective multicenter trial comparing repeated immunosuppressive therapy with stem-cell transplantation from an alternative donor as second-line treatment for children with severe and very severe aplastic anemia. *Blood.* 2008;111(3):1054-1059.

To the editor:

Peripheral blood stem cells versus bone marrow in pediatric unrelated donor stem cell transplantation

The relative benefits and risks of peripheral blood stem cells (PBSCs) versus bone marrow (BM) for allogeneic hematopoietic stem cell transplantation (SCT) are still a matter of highly controversial debates.[1-3] The first randomized study comparing the 2 stem cell sources in unrelated donor SCT recently documented comparable overall and event-free survival, but indicated a higher risk for chronic graft-versus-host disease (GVHD) with PBSCs.[4] Only a few pediatric patients were included in this study even though the long-term sequelae of chronic GVHD are of particular concern in this patient group.

We retrospectively compared the long-term outcome of contemporaneous unrelated donor SCT in 220 children transplanted with BM (n = 102) or PBSCs (n = 118) for hematologic malignancies and reported to the German/Austrian pediatric registry for SCT. All patients had received myeloablative conditioning followed by unmanipulated SCT from HLA-matched unrelated donors. The PBSC and BM groups were comparable with regard to patient and donor age, sex, cytomegalovirus (CMV) serostatus, disease status at transplantation, GVHD prophylaxis, growth factor use, and degree of HLA matching. The groups differed with regard to disease category with slightly more myelodysplastic syndrome patients (P = .02) and a higher CD34-cell dose (P = .001) in the PBSC group.

Neutrophil and platelet engraftment were achieved significantly faster after PBSC than BM transplantation (Figure 1A-B). In this entirely pediatric cohort, the incidence of clinically relevant grade

II-IV acute GVHD (Figure 1C) did not differ. Most importantly, the incidence of chronic GVHD (PBSCs vs BM: 35% vs 33%, respectively; P = .9) and extensive chronic GVHD (Figure 1D) proved low and was virtually identical in the 2 groups. With a median follow-up time of 3 years, overall survival (PBSCs vs BM: 50% ± 5% vs 46% ± 6%, respectively; P = .63) and event-free survival (PBSCs vs BM: 45% ± 5% vs 44% ± 6%, respectively; P = .59) were comparable (Figure 1E-F). In multivariable analysis, taking into account all parameters with P < .2 in univariate analysis, the only significant independent risk factor for treatment failure was advanced disease status at the time of transplantation (relative risk = 2.4, 95% confidence interval, 1.5-3.8; P = .001). In contrast, stem cell source (PBSCs vs BM) had no effect (relative risk = 1.1, 95% confidence interval, 0.7-1.6; P = .8).

Our registry-based analysis provides evidence that in pediatric recipients of HLA-matched unrelated-donor transplantation with consistent antithymocyte globulin (ATG) use during conditioning, transplantation with PBSCs and BM results in comparable clinical outcomes without detectable differences in the risk of acute or, more importantly, chronic GVHD. Consistent with a recent study underscoring the role of ATG for the prevention of acute and chronic GVHD,[5] the use of ATG in 96% of our transplantation procedures compared with only 27% in the above-mentioned randomized study by Anasetti et al[4] might be one of the key factors responsible for the overall low and comparable incidence of

Duodenal follicular lymphoma lacks AID but expresses BACH2 and has memory B-cell characteristics

Katsuyoshi Takata[1], Yasuharu Sato[1], Naoya Nakamura[2], Mami Tokunaka[2], Yukari Miki[3], Yara Yukie Kikuti[2], Kazuhiko Igarashi[4], Etsuro Ito[5], Hideo Harigae[6], Seiichi Kato[7], Eiko Hayashi[1], Takashi Oka[1], Yoshinobu Hoshii[8], Akira Tari[9], Hiroyuki Okada[10], Abd Alkader Lamia Mohamad[1], Yoshinobu Maeda[11], Mitsune Tanimoto[11], Tomohiro Kinoshita[12] and Tadashi Yoshino[1]

[1]Department of Pathology, Okayama University Graduate School of Medicine, Dentistry and Pharmaceutical Sciences, Okayama, Japan; [2]Department of Pathology, Tokai University School of Medicine, Isehara, Japan; [3]Department of Medical Technology, Kagawa Prefectural University of Health Sciences, Takamatsu, Japan; [4]Department of Biochemistry, Tohoku University Graduate School of Medicine, Sendai, Japan; [5]Department of Pediatrics, Hirosaki University Graduate School of Medicine, Hirosaki, Japan; [6]Division of Hematology and Rheumatology, Tohoku University Graduate School of Medicine, Sendai, Japan; [7]Department of Pathology and Laboratory Medicine, Nagoya University Hospital, Nagoya, Japan; [8]Department of Pathology, Yamaguchi University Graduate School of Medicine, Ube, Japan; [9]Division of Gastroenterology, Department of Internal Medicine, Hiroshima Red Cross Hospital and Atomic-Bomb Survivors Hospital, Hiroshima, Japan; [10]Department of Endoscopy, Okayama University Hospital, Okayama, Japan; [11]Department of Hematology, Oncology and Respiratory Medicine, Okayama University Graduate School of Medicine, Okayama, Japan and [12]Department of Hematology and Cell Therapy, Aichi Cancer Center, Nagoya, Japan

We have reported previously that duodenal follicular lymphoma (FL) is distinct from nodal FL and showed more resemblance to mucosa-associated lymphoid tissue lymphoma, and that FL frequently involved the duodenal second portion. In the present study, we examined duodenal FLs and gastric/colonic FLs to clarify the clinicopathological and immunological differences between the tumor types. We analyzed 8 samples of gastric FL, 17 of duodenal ones, and 5 of colonic/rectal ones, and characterized them by immunohistochemistry, immunogenotyping, and histology. Gastric and colonic FLs presented in submucosal to subserosal areas, whereas duodenal ones presented in the mucosal to submucosal layers. Immunohistochemical analysis revealed that duodenal FLs exhibited the following phenotypes: CD10 (+), B-cell lymphoma 2 (BCL-2) (+), BCL-6 (+), activation-induced cytidine deaminase (AID) (−), BACH2 (+), CD27 (+), MUM-1 (−), Blimp-1 (−), and loose CD21 network (duodenal pattern). Gastric/colonic FLs exhibited the following phenotypes: CD10 (+), BCL-2 (+), BCL-6 (+), AID (+), BACH2 (+), CD27 (−), MUM-1 (−), Blimp-1 (−), and a dense CD21 network (nodal pattern). Expression of AID and CD27 in lymphoma cells and the CD21 network pattern were considerably different between duodenal FLs and gastric/colonic ones. Moreover, in situ hybridization revealed that, in the duodenal FLs, BACH2 was expressed at the periphery of the tumor follicle and tumor villi. The number of immunoglobulin heavy-chain variable domains VH4 and VH5 were higher in duodenal follicular lymphomoas than in gastric FLs. The lymphoma cells of duodenal FLs are different from those of gastric/colonic FLs, and duodenal FL is distinct even within the gastrointestinal tract. Somatic hypermutation in immunoglobulin genes and CD27 expression are hallmarks of memory B cells. We suggest that duodenal FL cells are in the memory B-cell stage, and require BACH2 instead of AID for ongoing mutation.
Modern Pathology (2013) 26, 22–31; doi:10.1038/modpathol.2012.127; published online 17 August 2012

Keywords: BACH2; gastrointestinal follicular lymphoma; memory B cell

We have reported that duodenal follicular lymphoma (FL) is a distinct FL by virtue of lacking follicular dendritic cells (FDC), activation-induced cytidine deaminase (AID), and immunoglobulin variable heavy-chain deviation.[1,2] On the other hand, we have also reported that duodenal FLs harbor t(14;18)(IGH-BCL-2), exhibit ongoing somatic hypermutations, and express CD10 and B-cell lymphoma 2 (BCL-2), which are common features of nodal FL. However, the proteins have roles in somatic hypermutation in duodenal FL have not yet been identified.

Although the duodenal second portion is the most frequent site of FL in the gastrointestinal tract,[3,4] it sometimes occurs primarily in the gastrointestinal tract outside of the duodenum. Using double-balloon and/or capsule endoscopy, FLs of the gastrointestinal tract primarily involve the duodenum and frequently spread to the small intestine,[3] Few FLs occur in the stomach and colon, but the clinicopathological features of FL in such organs remain unclear. AID has a key role in class switching and somatic hypermutation in B cells,[5] and BACH2 also has a role in these processes in B cells.[6] BACH2 and Bcl-6 suppress Blimp-1, which is a key regulator of plasma-cell differentiation.[7] We have previously reported the lack of AID expression in duodenal FLs, but the entity associated with somatic hypermutation and ongoing mutation remains unknown. Therefore, we focused on BACH2 expression, especially in duodenal FLs, and sought to clarify the differences between duodenal and other gastrointestinal FLs with special reference to the characteristics of FDC, the expression of AID and BACH2, and stage of differentiation in lymphoma cells.

Materials and methods

Patients

Subjects included 8 patients with FL in the stomach, 5 with FL in the colon and rectum, and 17 with FL in the duodenum, which were previously reported.[1] We obtained three samples of reactive lymphoid hyperplasia of the lymph node and three of the duodenum for CD27 immunohistochemical control specimens. Informed consent to use the samples was obtained from all the patients.

Immunohistochemical Analysis

Immunohistochemical staining was performed on sections from 10% buffered formalin-fixed and paraffin-embedded tissues using heat-induced epitope retrieval or trypsin-induced retrieval, an avidin–biotin complex method, and an automated immunostainer (Ventana Medical System, Tuscon, AZ, USA), as previously described.[8] The antibody panel used to assess these cases was as follows (clone, dilution): CD20 (L26, 1:200), CD3 (PS-1, 1:50), CD10 (56C6, 1:50), CD5(4C7, 1:100), Bcl-2

(3.1, 1:200), CD23 (1B12, 1:100), CD27 (137B4, 1:50), and Ki-67 (MIB-1, 1:5000) (Novocastra, Newcastle-upon-Tyne, UK); CD21 (1F8, 1:20), MUM-1 (MUM1p, 1:50) (DAKO Cytomation, Denmark); Bcl-6 (D-8, 1:100) (Santa Cruz Biotechnology, Santa Cruz, CA, USA); cyclin D1 (SP4, ready to use) (Nichirei, Japan); AID (ZA001, 1:100) (Zymed, South San Francisco, CA, USA); and Blimp-1 (3H2-E8, 1:200) (Novus Biologicals, Littleton, CO, USA). Rabbit polyclonal anti-human BACH2 antibody (F69-2) was used as a primary antibody at a dilution of 1:500. Muto et al[6] recently reported that staining with the anti-BACH2 antibody was severely diminished in the spleens of BACH2-deficient mice, verifying the specificity of the antibody. For CD20, CD3, CD10, CD5, Cyclin D1, Bcl-2, Bcl-6, and MUM-1 antigens, samples were scored as positive when 30% or more of lymphoma cells were positively stained. For AID expression in tumor follicles, samples with 5% or more expressing cells were scored as positive as previously described.[9] Ki-67-positive cells were counted in tumor follicles. CD21 expression patterns were classified as follows: nodal (>30% positive cells); intermediate (5–30% positive cells); and duodenal (<5% positive cells and FDC located at the periphery of tumor follicles).

Fluorescence In Situ Hybridization (FISH)

FISH for t(14;18)(q32;q21)/IGH-BCL-2 translocations was performed using the LSI BCL-2 FISH DNA fusion signal probe (Abbott Molecular, Wiesbaden, Germany) according to the manufacturer's instructions. We performed FISH directly on paraffin-embedded tissue sections and detected the hybridization signal as previously described.[10]

In Situ Hybridization

In situ hybridization was performed on paraffin-embedded tissue sections using a BACH2 RNA probe, which was designed using a modified multi-labeling method as previously described.[11]

DNA Extraction and PCR

DNA was extracted from paraffin-embedded tissue using the QIAmp DNA Micro Kit (Qiagen, Valencia, CA, USA). The variable regions (CDR2 and FW3) and VDJ region (CDR3) of the immunoglobulin heavy-chain (IgVH) gene were amplified by semi-nested PCR, using the primers of FR2, LJH, and VLJH as described earlier.[1,12] Primers used were as follows: 5'-CCGGRAARRGTCTGGAGTGG-3', as upstream consensus V region primer (FR2); 5'-CTTACCTG AGGAGACGGTGACC-3', as a consensus J region primer (LJH); 5'-GTGACCAGGTNCCTTGGCCCC-3', as a consensus J region primer (VLJH). PCR products were purified using the QIAquick PCR purification

kit (Qiagen). Then, 1 μl of the PCR product was used for direct sequencing (ABI PRISM Model 3100, version 3.7, Applied Biosystems). Next, the resulting immunoglobulin sequence was fed into BLAST (NCBI) to identify the closest germline sequences.

Western Blotting

CD27 protein expression in tumor samples was determined by western blot analysis. Protein lysates were analyzed using standard techniques and the anti-CD27 rabbit polyclonal antibody (Abcam, Tokyo, Japan) as described.[13] We included one fresh-frozen reactive lymphoid hyperplasia sample as a positive control, a HeLa cell line sample as a negative control, and three fresh-frozen duodenal FL samples in each analysis.

Statistical Analysis

All statistical analyses were performed with the Mann–Whitney U-test using SPSS software (version 14.0; SPSS, Chicago, IL, USA). Values of $P < 0.05$ were considered statistically significant.

Results

Clinicopathological Findings

Clinical features (age, gender, and clinical stage), histological grading, and immunohistochemical

findings are summarized in Table 1. The study group comprised 16 men and 14 women, aged between 40 and 81 years, with a median age of 61 years (Stomach FL: age range, 51–81 years; median age, 63 years. Duodenum FL: age range, 49–75 years; median age, 61 years. Colon and rectum FL: age range, 40–87 years, median age, 58 years). Clinical stages were determined according to the criteria recommended by the International Workshop (Lugano) and are detailed in Table 1. All stage IV patients had bone marrow involvement. We excluded patients with multiple lymph node lesions. In our patient series, the stage IV patients had both gastrointestinal lesions and bone marrow lesions, and they had predominant gastrointestinal involvement. Typical histological appearance of patient samples showed a vague nodular pattern composed of small- to medium-sized cleaved lymphoid cells. The main locations of gastric and colonic FLs were the submucosal to subserosal areas (Figures 1a–f). Duodenal FLs were located in the submucosal area (Figures 1g–i), and tumor cells were associated with duodenal villi. Histological grades were distributed as follows: grade 1: 24 samples; grade 2: 5 samples; Grade 3A: 1 sample.

Immunophenotyping Results

CD21 expression patterns are shown in Table 2. FDC were arranged at the periphery of tumor follicles in

Table 1 Clinicopathological features in gastrointestinal FLs

Patient no.	Sites	Age (years)/gender	Stage	Grade	CD20	CD10	CD5	Cyclin D1	BCL-2	BCL-6	MUM-1	Blimp-1
1	Stomach	60/M	I	1	+	+	−	−	+	+	−	−
2	Stomach	75/M	IV	1	+	+	−	−	+	+	−	−
3	Stomach	63/M	I	1	+	+	−	−	+	+	−	−
4	Stomach	60/F	I	2	+	+	−	−	+	+	−	−
5	Stomach	51/F	II2	1	+	+	−	−	+	+	−	−
6	Stomach	81/F	I	2	+	+	−	−	+	+	−	−
7	Stomach	51/F	I	2	+	+	−	−	±	+	−	−
8	Stomach	74/M	II1	1	+	+	−	−	+	+	−	−
9	Duodenum	75/M	I	1	+	+	−	−	+	+	−	−
10	Duodenum	57/M	I	1	+	+	−	−	+	+	−	−
11	Duodenum	58/M	IV	1	+	+	−	−	+	+	−	−
12	Duodenum	75/M	II2	1	+	+	−	−	+	+	−	−
13	Duodenum	71/F	I	1	+	+	−	−	+	+	−	−
14	Duodenum	66/F	I	1	+	+	−	−	+	+	−	−
15	Duodenum	51/M	I	1	+	+	−	−	+	+	−	−
16	Duodenum	49/M	II2	1	+	+	−	−	+	+	−	−
17	Duodenum	62/F	II2	1	+	+	−	−	+	+	−	−
18	Duodenum	54/M	I	1	+	+	−	−	+	+	−	−
19	Duodenum	61/F	IV	1	+	+	−	−	+	+	−	−
20	Duodenum	53/F	II2	1	+	+	−	−	+	+	−	−
21	Duodenum	57/F	I	2	+	+	−	−	+	+	−	−
22	Duodenum	56/M	II2	1	+	+	−	−	+	+	−	−
23	Duodenum	66/F	II2	1	+	+	−	−	+	+	−	−
24	Duodenum	55/F	II2	1	+	+	−	−	+	+	−	−
25	Duodenum	63/F	II2	1	+	+	−	−	+	+	−	−
26	Cecum	42/M	II2	2	+	+	−	−	+	+	−	−
27	Colon	40/M	I	1	+	+	−	−	+	+	−	−
28	Colon	47/M	I	3A	+	+	−	−	+	+	−	−
29	Rectum	67/F	I	1	+	+	−	−	+	+	−	−
30	Rectum	77/M	I	1	+	+	−	−	+	+	−	−

Abbreviations: BCL-2, B-cell lymphoma 2; F, female; FL, follicular lymphoma; M, male.
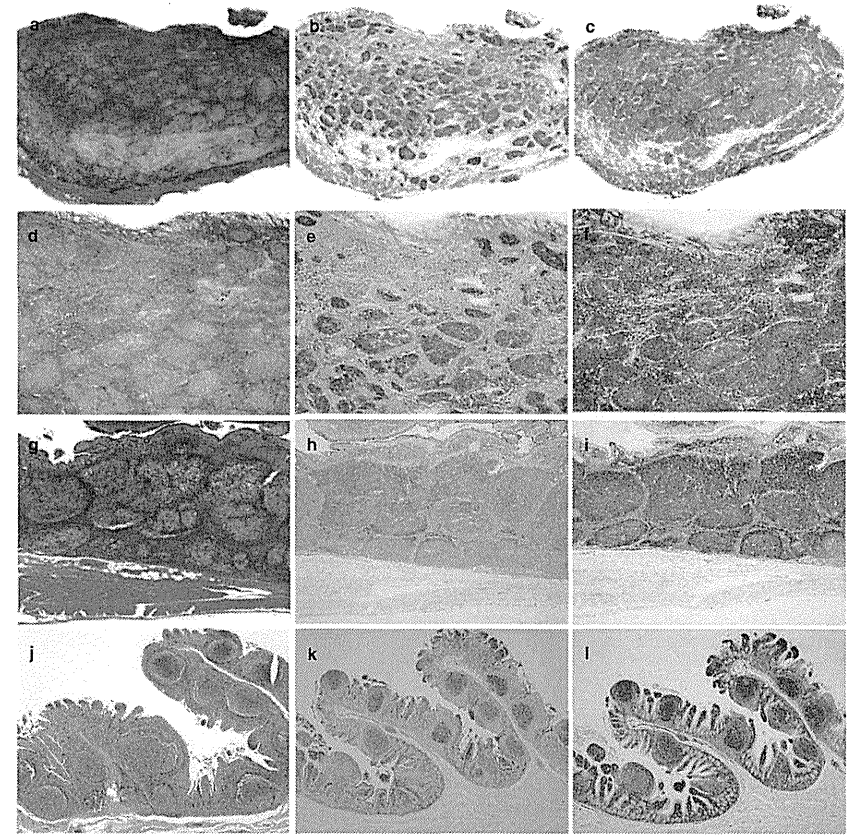
Figure 1 Pathological features of gastric, duodenal, and colonic/rectal follicular lymphoma (FL). (a) Gastric FL (HE stain; low power field). Tumor cells are present in the proper muscle to subserosal area. (b) CD10 immunostaining of gastric FL (low power field). (c) B-cell lymphoma 2 (BCL-2) immunostaining of gastric FL (low power field). (d) Gastric FL (HE. stain). Vague nodular tumor follicles are present. (e) CD10 immunostaining of gastric FL. Tumor cells are positive. (f) BCL-2 immunostaining of gastric FL. Tumor cells are positive. (g) Colonic FL (HE stain). Tumor cells are present in the musculature proper area. (h) CD10 immunostaining of colonic FL. Tumor cells are positive. (i) BCL-2 immunostaining of colonic FL. Tumor cells are positive. (j) Duodenal FL (HE stain). Tumor cells are present in the lamina propria area. (k) CD10 immunostaining of duodenal FL. Tumor cells are positive. (l) BCL-2 immunostaining of duodenal FL. Tumor cells are positive.

15 of 17 duodenal FLs as previously described (Figure 2a.[1] In contrast, among the eight stomach FLs, seven exhibited a nodal pattern and one showed an intermediate pattern (Figure 2b). Out of five patient samples in the colon and rectum, three were nodal and two were intermediate (Figures 2c and d). Statistical comparison of the expression patterns of duodenal FLs and gastric/colonic FLs

showed that the distributions were significantly different ($P < 0.001$).

Results of AID and BACH2 expression analyses are also shown in Table 2. Only 1 of 17 duodenal FLs expressed AID (Figure 2e), whereas 6 of 8 gastric FLs were positive for AID (Figure 2f). All colonic and rectal samples were positive for AID. BACH2 expression was comparatively different: 14 of 17

Table 2 CD21 pattern, AID, BACH2 expression and genetical study in gastrointestinal follicular lymphomas

Patient no.	Sites	Stage	CD21 pattern	AID	BACH2	CD27	t(14;18)	VH usage
1	Stomach	I	Nodal	−	+	−	+	ND
2	Stomach	IV	Intermediate	+	+	−	+	VH3-30
3	Stomach	I	Nodal	+	−	−	−	VH3-21
4	Stomach	I	Nodal	+	+	−	−	VH3-30
5	Stomach	II2	Nodal	−	+	−	+	ND
6	Stomach	I	Nodal	+	+	−	−	VH3-7
7	Stomach	I	Nodal	+	+	+	−	VH3-30
8	Stomach	II1	Nodal	+	−	−	−	VH4-34
9	Duodenum	I	Duodenal	−	−	+	ND	VH3-73
10	Duodenum	I	Duodenal	−	−	+	ND	VH3-48
11	Duodenum	IV	Duodenal	−	+	−	+	VH3-72
12	Duodenum	II2	Duodenal	−	+	+	−	VH4-34
13	Duodenum	I	Duodenal	−	(+)	+	+	VH5-a
14	Duodenum	I	Nodal	−	+	+	−	VH3-73
15	Duodenum	I	Duodenal	−	(+)	+	+	VH4-b
16	Duodenum	II2	Duodenal	−	(+)	+	+	VH4-39
17	Duodenum	II2	Duodenal	+	−	+	+	VH3-15
18	Duodenum	I	Duodenal	−	(+)	+	+	VH5-51
19	Duodenum	IV	Duodenal	−	+	−	+	VH5-51
20	Duodenum	II2	Duodenal	−	(+)	+	+	VH4-61
21	Duodenum	I	Duodenal	−	(+)	+	+	VH4-39
22	Duodenum	II2	Duodenal	−	+	+	+	VH3-73
23	Duodenum	II2	Duodenal	−	(+)	+	+	VH3-23
24	Duodenum	II2	Nodal	−	+	+	+	VH3-23
25	Duodenum	II2	Duodenal	−	+	+	+	VH3-23
26	Cecum	II2	Nodal	+	+	+	−	ND
27	Colon	I	Intermediate	+	+	−	+	ND
28	Colon	I	Nodal	+	−	−	+	VH3-33
29	Rectum	I	Intermediate	+	+	−	−	ND
30	Rectum	I	Nodal	+	−	−	+	ND

Abbreviation: AID, activation-induced cytidine deaminase; ND, not determined.
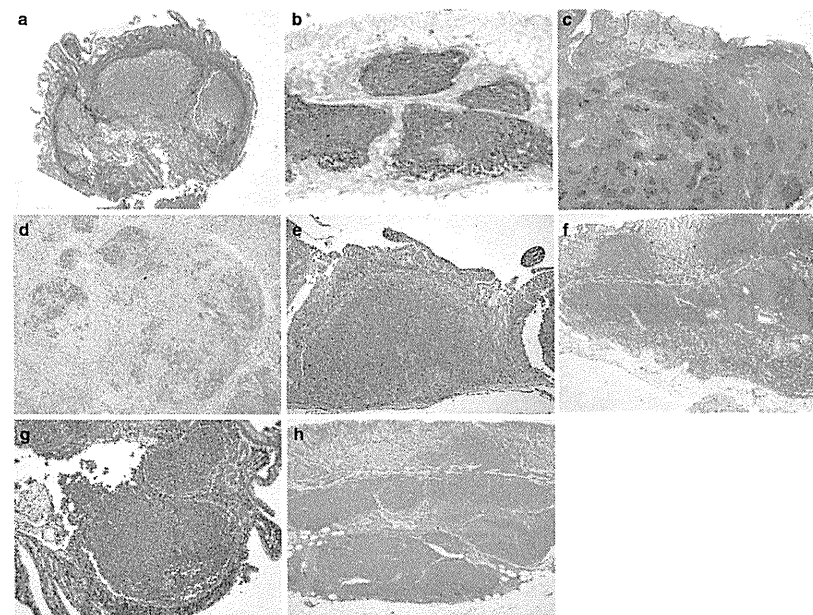(+): positive at the periphery of tumor follicle and villi.

Figure 2 CD21 and AID immunohistochemistry in duodenal, gastric, and colonic FLs. (a) CD21 immunostaining of duodenal FL. Follicular dendritic cells (FDC) present at the periphery of tumor follicles (duodenal pattern). (b) CD21 immunostaining of gastric FL. FDC networks densely present in tumor follicles (nodal pattern). (c) CD21 immunostaining of colonic FL. FDC networks densely present in tumor follicles (nodal pattern). (h) Intermediate pattern of CD21 immunostaining in colonic FL. (e) AID immunostaining in duodenal FL. Tumor cells are negative. (f) AID immunostaining of gastric FL. Tumor cells are positive. (g) BACH2 immunostaining in duodenal FL. Periphery of tumor follicles and villi are positive, but center of tumor follicle is negative. (h) BACH2 immunostaining of gastric FL. Tumor follicles are positive.

duodenal FL samples were positive for BACH2. Interestingly, the AID-positive sample (no. 20) was negative for BACH2. In seven samples, BACH2 was expressed at the periphery of the tumor follicle and tumor villi (Figure 2g, Table 2; shown as (+)). BACH2 was also commonly expressed in other FLs: six of eight gastric FLs were positive for BACH2 (Figure 2h) as were three of five colonic/rectal FLs.

In situ hybridization analysis of BACH2 expression confirmed the immunohistochemical findings. Tumor cells at the peripheral zone of tumor follicles and at the villi expressed BACH2 mRNA (Figures 3a and b). This pattern corresponded with the protein expression pattern. We also examined Blimp-1 expression and found no Blimp-1 expression in any of the patient samples (Table 2).

We examined differentiation in lymphoma cells using CD27 staining. As both mutated IgM+ B-cell populations and the class-switched memory B cells share expression of the TNF-receptor superfamily member CD27, which is not expressed in unmutated naive B cells,[14,15] CD27 is thought to be a memory B-cell marker.[16] Figure 3c shows CD27 expression in the reactive lymphoid hyperplasia of the duodenum: the CD27-positive B cells or plasma cells were present at the villi and lymphoid follicle. CD27 expression is also shown in the reactive hyperplastic germinal centers of the tonsil: the positive cells

were scattered in the germinal center (prominent in light zone) and interfollicular zone (Figure 3d).

As shown in Table 2, 15 of 17 duodenal FL samples strongly expressed CD27 (Figure 3e). Western blotting analysis also confirmed CD27 protein expression in duodenal FL (Supplementary Figure 1). In eight gastric and seven colonic FL samples, all samples were negative for CD27 (Figure 3f), except those of patients no. 7 and no. 26. Statistical comparison of expression patterns in duodenal FLs and nodal, gastric, and colon FLs showed that the distributions are significantly different ($P < 0.001$).

IgVH Gene Usage

We could detect monoclonal bands in six of eight gastric FL samples and one of five colonic/rectal FL samples. These results are shown in Table 2. In gastric FL, five of six were VH3 and one was VH4. In duodenal FL, 9 of 17 were VH3, 5 were VH4, and 3 were VH5.

Fluorescence In Situ Hybridization

The t(14;18) translocation was detected in 13 of 15 (about 87%) duodenal FL samples, 3 of 8 (38%) gastric FLs, and 3 of 5 (60%) colon and rectal FLs (Figure 4a). In gastric FL samples, the frequency of the

translocation was significantly lower than that in duodenal FLs ($P = 0.015$). Furthermore, gastric FLs with lower clinical stages (Stage I–II₁, localized tumor stage) had a lower tendency to exhibit the t(14;18) translocation (Table 2). The *IGH-BCL-2* translocation was more frequent in duodenal samples (87%) than in gastric (40%) and colonic (59%) FLs ($P = 0.008$).

Discussion

Although the gastrointestinal FLs are relatively rare, accounting for 1–3.6% of all gastrointestinal lymphomas, duodenal FLs have recently been found with increasing frequency by upper gastrointestinal endoscopic examination. These FLs are characterized by lower clinical stage, lower histological grading, and better prognosis. Gine et al[17] reported that the frequency of clinical stage III–IV in nodal FL was 81%. Solal-Celigny et al[18] found a similar frequency of 78%. In our previous multicenter

retrospective study, 41 of 191 patients with gastrointestinal FL (21.5%) were stage IV.[4] Histological differences between duodenal FLs and stomach and colon FLs involved tumor depth, size of individual tumor follicles and the size of the lesions. Duodenal FLs were mainly located in submucosal areas, and tumor cells were present in mucosal villi. Macroscopically, duodenal FLs typically present as small white multiple nodules. These histological differences suggest the association of a mucosal homing receptor such as $\alpha 4\beta 7$ as reported by Bende et al.[19] Most duodenal lymphoma samples are obtained by biopsy, and the assessment thus performed is considered insufficient. However, in our previous patient series, a few patients were examined by ultrasonic endoscopy. All patients who had macroscopically multiple white nodules had a limited submucosal layer. In our present series of duodenal FLs, all macroscopic types were found to be typical multiple white nodules. The patients in the present series were examined by CT and/or MRI.
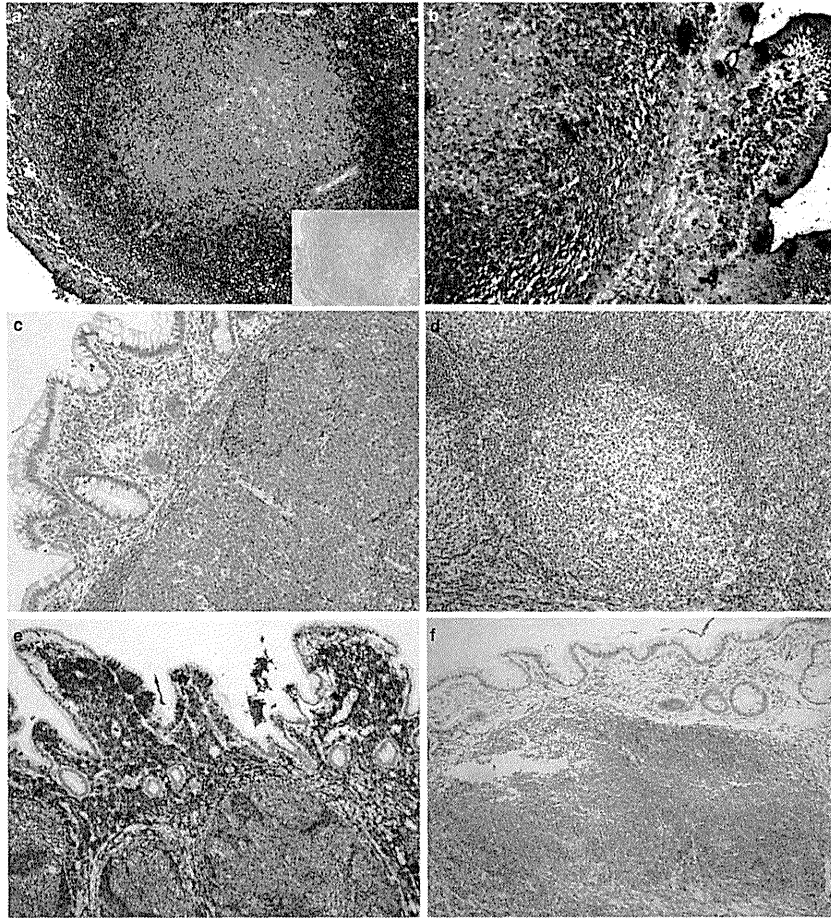
Figure 3 BACH2 and CD27 expression. (a) BACH2 *in situ* hybridization in duodenal follicular lymphoma (FL) sample. Levels of mRNA expression correlate with protein expression. Inset of Figure 3a shows detection of BACH2 mRNA with sense DIG-labeled probes as a negative control. (b) Same sample as Figure 3a. Tumor at the villi also expresses BACH2 at the mRNA level. (c) CD27 expression in reactive lymphoid hyperplasia of the duodenal sample. Positive cells (active B cells and plasma cells) are present at the villi. (d) CD27 immunostaining of reactive lymphoid hyperplasia in the tonsil sample. Positive cells are scattered in the germinal center light zone and interfollicular zone. (e) CD27 expression in duodenal FL. Tumor cells are strongly positive. (f) CD27 expression in colonic FL. Tumor follicles are negative.

We think we should examine further studies in the future.

Both normal germinal centers and nodal FLs have dense CD21-positive follicular dendritic cell networks.[20] We previously showed that duodenal FL lacked follicular dendritic cell networks, with dendritic cells distributed at the periphery of the tumor follicles.[1] In contrast, other gastrointestinal
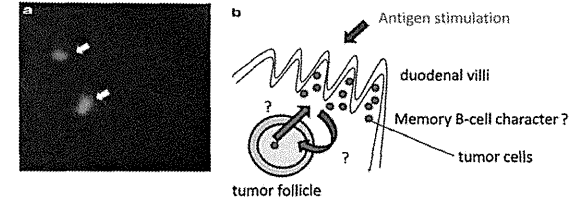
Figure 4 Fluorescence *in situ* hybridization (FISH) and schema of duodenal FL. (a) FISH for detection of t(14;18) in duodenal follicular lymphoma (FL) sample. IGH signal (green) and B-cell lymphoma 2 (BCL-2) signal (red) are merged (yellow: arrows). (b) Schema of tumor origin in duodenal FL.

tract (stomach, colon, and rectum) FLs had dense follicular dendritic cell networks similar to those of nodal FLs. The follicular dendritic cell network pattern may depend on the nature of the primary tumor. For example, we documented a patient with primary FL in the inguinal lymph node, who achieved complete remission by chemotherapy and then relapsed with lesions at duodenal and gastric sites. Interestingly, the nodal and two gastrointestinal sites showed the same follicular dendritic cell pattern (nodal pattern, data not shown). Conversely, some duodenal and nodal samples from patients presenting with systemic lymphadenopathy showed the same dendritic cell pattern (duodenal pattern, data not shown).

An important question concerns whether tumor cells invading the villi arise from the villi or whether they spread from tumor follicles to the villi. Figure 4b presents a hypothetical schema of development of duodenal FL. The VH-usage deviation and memory-cell characters strongly suggested that the presence of antigen stimulation, chemokines, and adhesion molecules probably affect tumor spreading. One hypothesis is that tumor cells originating in the villi spread to other villi and invade non-tumor follicles. Tumor cells invading non-tumor follicles disrupt the follicular dendritic cell network, as seen in follicular colonization in MALT lymphoma. Another hypothesis is that lymphoma cells from tumor follicles spread to the villi.

AID has a key role in class switching and somatic hypermutation in B cells.[5] BACH2 also has a role in these processes in B cells.[6] BACH2 and Bcl-6 suppress Blimp-1, which is a key regulator of plasma-cell differentiation.[7] We have previously reported a lack of AID expression in duodenal FLs. In the present study, 14 of 17 samples of duodenal FL expressed BACH2 protein and mRNA. In seven samples, the BACH2 pattern and the pattern of tumor cells in the villi and periphery of the tumor follicles was the same. This unique pattern was not found in nodal, gastric, or colonic FLs. This difference was quite interesting, but the mechanism by which AID and BACH2 are differentially expressed remains unclear. We cannot clearly demonstrate this

association in our present study, and further studies will be required to clarify this association.

Most duodenal follicular samples expressed BACH2, and all lacked Blimp-1, which is repressed by BACH2 and Bcl-6. Thus, BACH2 might have a key role in ongoing somatic hypermutation in duodenal FLs. Sakane-Ishikawa *et al*[21] described better prognostic value of BACH2 expression in diffuse large B-cell lymphomas. Takakuwa *et al*[22] described an inhibitory effect of BACH2 on proliferation of Raji cell lines. In previous reports, BACH2 was reported to have a tumor suppressor role in B-cell lymphomas. On the other hand, AID is associated with lymphomagenesis and AID expression is related to poor prognosis in several B-cell lymphoma subtypes.[9,23,24] We do not have sufficient data for long-term follow-up of patients with duodenal FL, but based on these reports, we suggest that BACH2 expression and lack of AID expression might limit the tumor stage and lead to better prognosis in duodenal FL.

Expression of CD27 was common (15 of 17) in the duodenal FL samples. In 16 Grade 1 nodal FLs, all patient samples were negative for CD27 (data not shown). In five gastric MALT lymphoma patient samples, four samples were positive and one was negative for CD27 (data not shown). In B-cell differentiation, postgerminal center B cells, selected by affinity maturation and induced by somatic hypermutation, differentiate to plasmablasts or memory B cells.[25] CD27 is a tumor necrosis factor receptor superfamily member and a general human memory B-cell marker. In human normal intestinal mucosa, scattered secretory IgA+ CD27+ memory B cells are present in the lamina propria, but are scarce in gut-associated lymphoid tissue.[26] In duodenal FL samples, tumor cells expressed IgA, CD27, and BACH2. Thus, tumor cells differentiate to memory B cells with somatic and ongoing hypermutations. For this reason, we note that these data suggest a resemblance of duodenal FL to MALT lymphoma. CD27+ memory B cells are subclassified as IgM+IgD+, IgM+IgD-, IgG+IgA+, and IgM-IgD+.[27] Thus, duodenal FLs are subclassified as IgA+ memory B-cell like. Dong HY *et al*[28] described that

CD27 did not distinguish between neoplastic B cells of naive *versus* memory type. Furthermore, Schmitter D *et al*[29] described CD27 expression in CD70-stimulated FL cells. Somatic hypermutation by itself is a feature of both follicular center and memory B cells, and CD27 is also expressed by some follicular center cells. Therefore, we should be more conservative in the precise maturational state of the duodenal FL cells. However, there might also be difference between nodal FL and duodenal FL in terms of CD27 expression.

In gastric and colonic FLs, *VH3* gene usage was frequently observed, but in our samples, we could detect too few monoclonal bands to allow comparison with duodenal samples. More samples will be required to compare VH gene usage. Translocations of t(14;18)(q32;q21) and *IGH-BCL-2* are considered to be hallmarks of FL,[29,30] but t(14;18) is present in about half the healthy samples.[31,32] In gastric FL of lower clinical stage, there were no IGH/BCL-2 translocations. These facts suggest that gastric FL may be similar to primary cutaneous follicle center lymphoma.[33,34]

In conclusion, we suggest that duodenal FL is a distinct entity among gastrointestinal FLs, by virtue of AID loss but BACH2 expression, displaying a specific CD21 pattern, and high frequency of CD27 expression.

Disclosure/conflict of interest

The authors declare no conflict of interest.

References

1 Takata K, Sato Y, Nakamura N, *et al*. Duodenal and nodal follicular lymphomas are distinct: the former lacks activation-induced cytidine deaminase and follicular dendritic cells despite ongoing somatic hypermutations. Mod Pathol 2009;22:940–949.

2 Sato Y, Ichimura K, Tanaka T, *et al*. Duodenal follicular lymphomas share common characteristics with mucosa-associated lymphoid tissue lymphomas. J Clin Pathol 2008;61:377–381.

3 Kodama M, Kitadai Y, Shishido T, *et al*. Primary follicular lymphoma of the gastrointestinal tract: a retrospective case series. Endoscopy 2008;40:343–346.

4 Takata K, Okada H, Ohmiya N, *et al*. Primary gastrointestinal follicular lymphoma involving the duodenal second portion is a distinct entity: A multicenter, retrospective analysis in Japan. Cancer Sci 2011;102:1532–1536.

5 Muramatsu M, Kinoshita K, Fagarasan S, *et al*. Class switch recombination and hypermutation require activation-induced cytidine deaminase (AID), a potential RNA editing enzyme. Cell 2000;102:553–563.

6 Muto A, Tashiro S, Nakajima O, *et al*. The transcriptional programme of antibody class switching involves the repressor BACH2. Nature 2004;429:566–571.

7 Igarashi K, Ochiai K, Muto A. Architecture and dynamics of the transcription factor network that regulates B-to-plasma cell differentiation. J Biochem 2007;141:783–789.

8 Khoury JD, Jones D, Yared MA, *et al*. Bone marrow involvement in patients with nodular lymphocyte predominant Hodgkin lymphoma. Am J Surg Pathol 2004;28:489–495.

9 Leuenberger M, Frigerio S, Wild PJ, *et al*. AID protein expression in chronic lymphocytic leukemia/small lymphocytic lymphoma is associated with poor prognosis and complex genetic alterations. Mod Pathol 2010;23:177–186.

10 Takada S, Yoshino T, Taniwaki M, *et al*. Involvement of the chromosomal translocation t(11;18) in some mucosa-associated lymphoid tissue lymphomas and diffuse large B cell lymphomas of the ocular adnexa: evidence from multiplex reverse transcriptase –polymerase chain reaction and fluorescence in situ hybridization on using formalin-fixed, paraffin embedded specimens. Mod Pathol 2003;16:445–452.

11 Mori H, Nomura T, Seno M, *et al*. Expression of phospholipid hydroperoxide glutathione peroxidase (PHGPx) mRNA in rat testes. Acta Histochem Cytochem 2001;34:25–30.

12 Nakamura N, Kuze T, Hashimoto Y, *et al*. Analysis of the immunoglobulin heavy chain gene variable region of CD5-positive and –negative diffuse large B cell lymphoma. Leukemia 2001;15:452–457.

13 Gajjar A, Hernan R, Kocak M, *et al*. Clinical, histopathologic, and molecular markers of prognosis: toward a new disease risk stratification system for medulloblastoma. J Clin Oncol 2004;22:984–993.

14 Agematsu K, Nagumo FC, Yang FC, *et al*. B cell subpopulations separated by CD27 and crucial collaboration of CD27+ B cells and helper T cells in immunoglobulin production. Eur J Immunol 1997;27:2073–2079.

15 Klein U, Rajewsky K, Kuppers R. Human immunoglobulin IgM + IgD + peripheral blood B cells expressing the CD27 cell surface antigen carry somatically mutated variable region genes: CD27 as a general marker for somatically mutated (memory) B cells. J Exp Med 1998;188:1679–1689.

16 Seifert M, Kuppers R. Molecular footprints of a germinal center derivation of human IgM + (IgD +) CD27 + B cells and the dynamics of memory B cell generation. J Exp Med 2009;16:2659–2669.

17 Gine E, Montoto S, Bosch F, *et al*. The follicular lymphoma international prognostic index (FLIPI) and the histological subtype are the most important factors to predict histological transformation in follicular lymphoma. Ann Oncol 2006;17:1539–1545.

18 Solal-Celigny P, Roy P, Colombat P, *et al*. Follicular lymphoma international prognostic index. Blood 2004;1:1258–1265.

19 Bende RJ, Smit LA, Bossenbroek JG, *et al*. Primary follicular lymphoma of the small intestine: alpha4beta7 expression and immunoglobulin configuration suggest an origin from local antigen-experienced B cells. Am J Pathol 2003;162:105–113.

20 Kagami Y, Jung J, Choi YS, *et al*. Establishment of a follicular lymphoma cell line (FLK-1) dependent on follicular dendritic cell line HK. Leukemia 2001;15:148–156.

21 Sakane-Ishikawa E, Nakatsuka S, Tomita Y, *et al*. Prognostic significance of BACH2 expression in diffuse large B-cell lymphoma: A study of the Osaka lymphoma study group. J Clin Oncol 2005;23:8012–8017.

22 Takakuwa T, Luo WJ, Ham MF, *et al*. Integration of Epstein-Barr virus into chromosome 6q15 of Burkitt lymphoma cell line (Raji) induces loss of BACH2 expression. Am J Pathol 2004;164:967–974.

23 Gu X, Shivarov V, Strout MP. The role of activation-induced cytidine deaminase in lymphomagenesis. Curr Opin Hematol 2012;19:292–298.

24 Dijkman R, Tensen CP, Buettner M, *et al*. Primary cutaneous follicle center lymphoma and primary cutaneous large B-cell lymphoma, leg type, are both targeted by aberrant somatic hypermutation but demonstrate differential expression of AID. Blood 2006;107:4926–4929.

25 Allen CDC, Okada T, Cyster JG. Germinal-center organization and cellular dynamics. Immunity 2007;27:190–202.

26 Brandtzaeg P, Johansen FE. Mucosal B cells: phenotypic characteristics, transcriptional regulation, and homing properties. Immunol Rev 2005;206:32–63.

27 Berkowska MA, Driessen GJA, Bikos V, *et al*. Human memory B cells originate from three distinct germinal center-dependent and –independent maturation pathways. Blood 2011;118:2150–2158.

28 Dong HY, Shahasafaei A, Dorfman DM. CD148 and CD27 are expressed in B cell lymphomas derived from both memory and naïve B cells. Leuk Lymphoma 2002;43:1855–1858.

29 Schmitter D, Bolliger U, Hallek M, *et al*. Involvement of the CD27-CD70 co-stimulatory pathway in allogenic T-cell response to follicular lymphoma cells. Br J Haematol 1999;106:64–70.

30 Helen MC, David BJ, Dennis HW. Cytogenetic and molecular studies of t(14;18) and t(14;19) in nodal and extranodal B-cell lymphoma. J Pathol 1992;166:129–137.

31 Albinger-Hegyi A, Hochreutener B, Abdou MT, *et al*. High frequency of t(14;18)-translocation breakpoints outside of major breakpoints and minor cluster regions in follicular lymphomas. Am J Pathol 2002;160:823–832.

32 Hirt C, Dölken G, Janz S, *et al*. Distribution of t(14;18)-positive, putative lymphoma precursor cells among B-cell subsets in healthy individuals. Br J Haematol 2007;138:349–353.

33 Roulland S, Navarro JM, Grenot P, *et al*. Follicular lymphoma-like B cells in healthy individuals: a novel intermediate step in early lymphomagenesis. J Exp Med 2006;203:2425–2431.

34 Streubel B, Scheucher B, Valencak J, *et al*. Molecular cytogenetic evidence of t(14;18)(IGH;BCL2) in a substantial proportion of primary cutaneous follicle center lymphomas. Am J Surg Pathol 2006;30:529–536.

Supplementary Information accompanies the paper on Modern Pathology website (http://www.nature.com/modpathol)